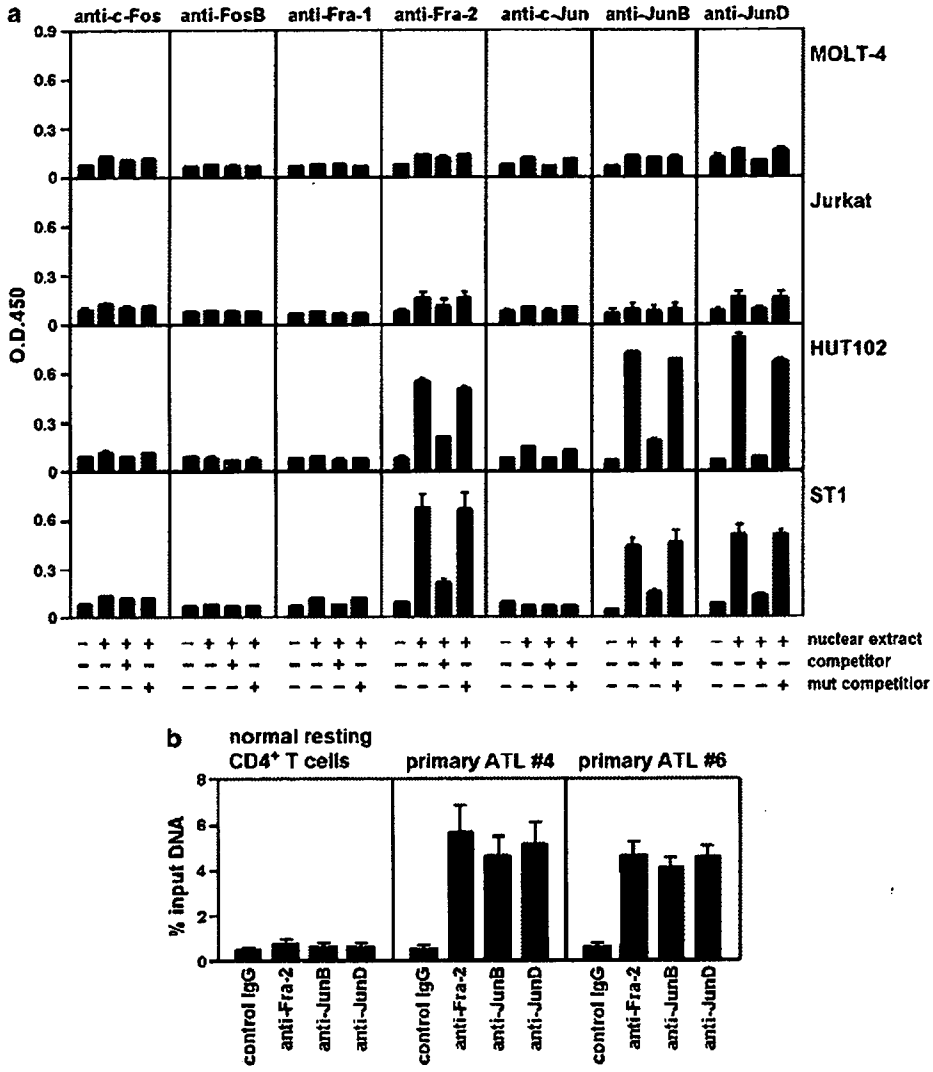

Figure 4 Specific binding of Fra-2, JunB and JunD to the AP-1 site in the CCR4 promoter. (a) NoShift assay. Nuclear extracts were prepared from two control T-cell lines (MOLT-4 and Jurkat) and two adult T-cell leukemia (ATL) cell lines (HUT102 and ST1). Nuclear proteins that bound to the biotinylated AP-1 site oligonucleotide (TGGGAAATGACTAAGAATCAT) were captured on an avidin-coated plate and detected by anti-c-Fos, anti-FosB, anti-Fra-1, anti-Fra-2, anti-c-Jun, anti-JunB or anti-JunD, as indicated. Specificity was determined by adding unlabeled probe (competitor; TGGGAAATGACTAAGAATCAT) or mutant probe (mut competitor; TGGGAAATGTCAAAGAATCAT; differences underlined). Each bar represents the mean ± s.e.m. from three separate experiments. (b) Chromatin immunoprecipitation (ChIP) assay. Chromatins from normal CD4+ T cells from healthy donors (purity, >96%) and primary ATL cells from two patients (leukemic cells, >90%) were immunoprecipitated with anti-Fra-2, anti-JunD or control IgG. The amounts of precipitated DNA relative to total input DNA were quantified by real-time PCR for the CCR4 promoter region containing the AP-1 site. Each bar represents the mean ± s.e.m. from three separate experiments.

Identification of downstream target genes of the Fra-2/JunD heterodimer in ATL cells

To identify the target genes of Fra-2 in ATL cells, we compared the gene expression profiles of ATL-derived ST1 cells transfected with Fra-2 siRNA or control siRNA using the Affymetrix high-density oligonucleotide microarray. As summarized in Figure 6a, at least 49 genes were downregulated more than threefold by Fra-2 siRNA. The classification of these genes according to their biological functions shows that Fra-2 promotes the expression of genes involved in signal transduction (10 genes), protein biosynthesis and modification (8 genes) and transcription (6 genes); it also stimulates the expression of 10 genes of unknown function. Most notably, the list includes the proto-oncogenes c-Myb, BCL-6 and MDM2 (Oh and Reddy, 1999; Pasqualucci *et al*., 2003; Vargas *et al*., 2003). As shown in Figure 6b, RT–PCR analysis verified that not only Fra-2 siRNA but also JunD siRNA downregulated these proto-oncogenes in two ATL cell lines. Therefore, c-Myb, BCL-6 and MDM2 are the downstream target genes of the Fra-2/JunD heterodimer in both cell lines. This prompted us to examine the expression of c-Myb, BCL-6 and MDM2 in freshly isolated primary ATL cells by

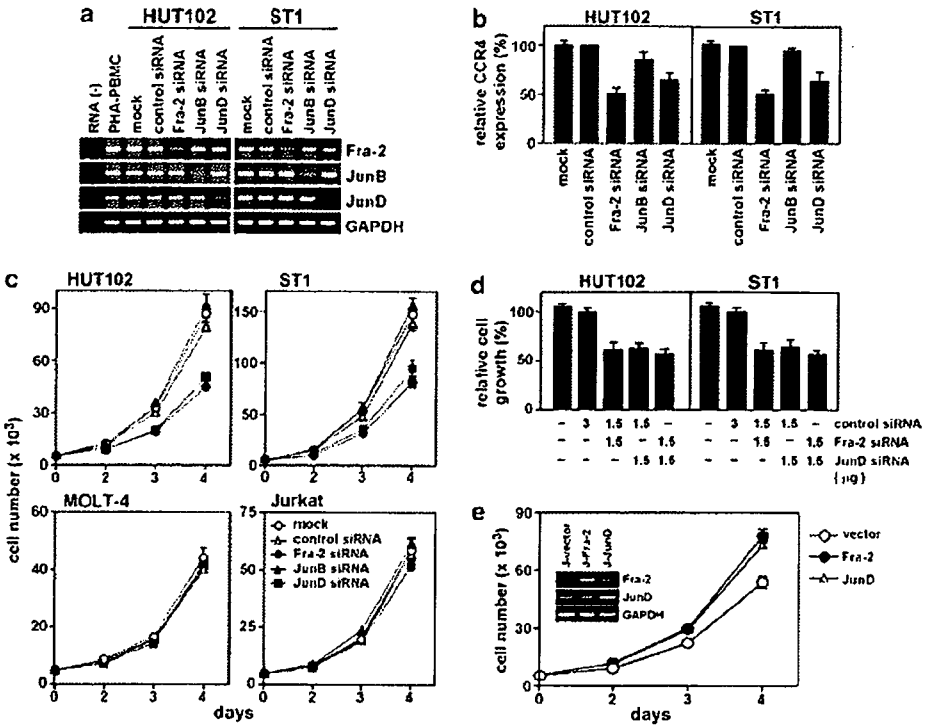

Figure 5 Dominant role of Fra-2/JunD in CCR4 expression and cell proliferation in adult T-cell leukemia (ATL). (a) Reverse transcription (RT)–PCR analysis to determine the effect of siRNAs. HUT102 and ST1 were transfected with control siRNA or siRNA for Fra-2, JunB or JunD. After 48 h, total RNA was prepared. The representative results from three separate experiments are shown. (b) Real-time RT–PCR analysis for CCR4 expression. HUT102 and ST1 were transfected with control siRNA or siRNA for Fra-2, JunB or JunD. After 48 h, total RNA was prepared and real-time RT–PCR was performed for CCR4 and 18S ribosomal RNA (an internal control). Data are presented as the mean ± s.e.m. of three separate experiments. (c) Effect of siRNAs on cell growth. HUT102, ST1, MOLT-4 and Jurkat were transfected with control, Fra-2, JunB and JunD siRNAs and cultured in a 96-well plate at 0.5×10^4 cells per well. At the indicated time points, viable cell numbers were determined using a FACSCalibur by gating out cells stained with propidium iodide. Data are shown as the mean ± s.e.m. of three separate experiments. (d) Effect of double knockdown of Fra-2 and JunD on cell growth. HUT102 and ST1 were transfected with control, Fra-2 and JunD siRNAs as indicated and cultured in a 96-well plate at 0.5×10^4 cells per well. At 4 days, viable cell numbers were determined on a FACSCalibur by gating out dead cells stained with propidium iodide. Data are shown as the mean ± s.e.m. of three separate experiments. (e) Effect of stable expression of Fra-2 and JunD on cell growth. Jurkat cells were transfected with a control IRES-EGFP expression vector or an IRES-EGFP expression vector for Fra-2 or JunD. Stable transfectants expressing green fluorescence protein were sorted and cultured in a 96-well plate at 0.5×10^4 cells per well. At the indicated time points, viable cell numbers were determined on a FACSCalibur by gating out dead cells stained with propidium iodide. Data are shown as the mean ± s.e.m. of three separate experiments.

RT–PCR. As shown in Figure 6c, we indeed detected the constitutive expression of c-Myb, BCL-6 and MDM2 at high levels in primary ATL cells. In sharp contrast, normal resting $CD4^+$ T cells hardly expressed these proto-oncogenes.

Discussion

The AP-1 transcription factors function as homodimers or heterodimers formed by Jun (c-Jun, JunB and JunD), Fos (c-Fos, FosB, Fra-1 and Fra-2) and the ATF family proteins (Shaulian and Karin, 2002; Eferl and Wagner, 2003). Most of them are rapidly and transiently induced by extracellular stimuli that trigger the activation of the Janus kinase (JNK), extracellular signal regulated protein kinases 1 and 2 (ERK1/2) or p38 mitogen-activated protein (MAP) kinase pathways (Shaulian and Karin, 2002; Eferl and Wagner, 2003). The AP-1 family is known to be involved in cellular proliferation, oncogenesis and even tumor suppression, depending on the combination of AP-1 proteins and the cellular context (Shaulian and Karin, 2002; Eferl and Wagner, 2003). Previously, by using the AP-1 site of the IL-8 promoter, Mori *et al.* demonstrated a strong Tax-independent expression of JunD in primary ATL cells (Mori *et al.*, 2000). In the present study, we have shown that Fra-2 is constitutively expressed at high levels in primary ATL cells (Figure 2a). Furthermore, except for JunB and JunD, other members of the AP-1 family are mostly negative in primary ATL cells (Figure 2a). Therefore, as demonstrated in the present study, the Fra-2/JunD and Fra-2/JunB heterodimers may be the major AP-1 factors constitutively active in primary ATL cells.

It has been shown that HTLV-1 Tax induces the expression of various AP-1 family members such as c-Fos, Fra-1, c-Jun and JunD (Nagata *et al.*, 1989; Iwai *et al.*, 2001). We indeed observed the expression of

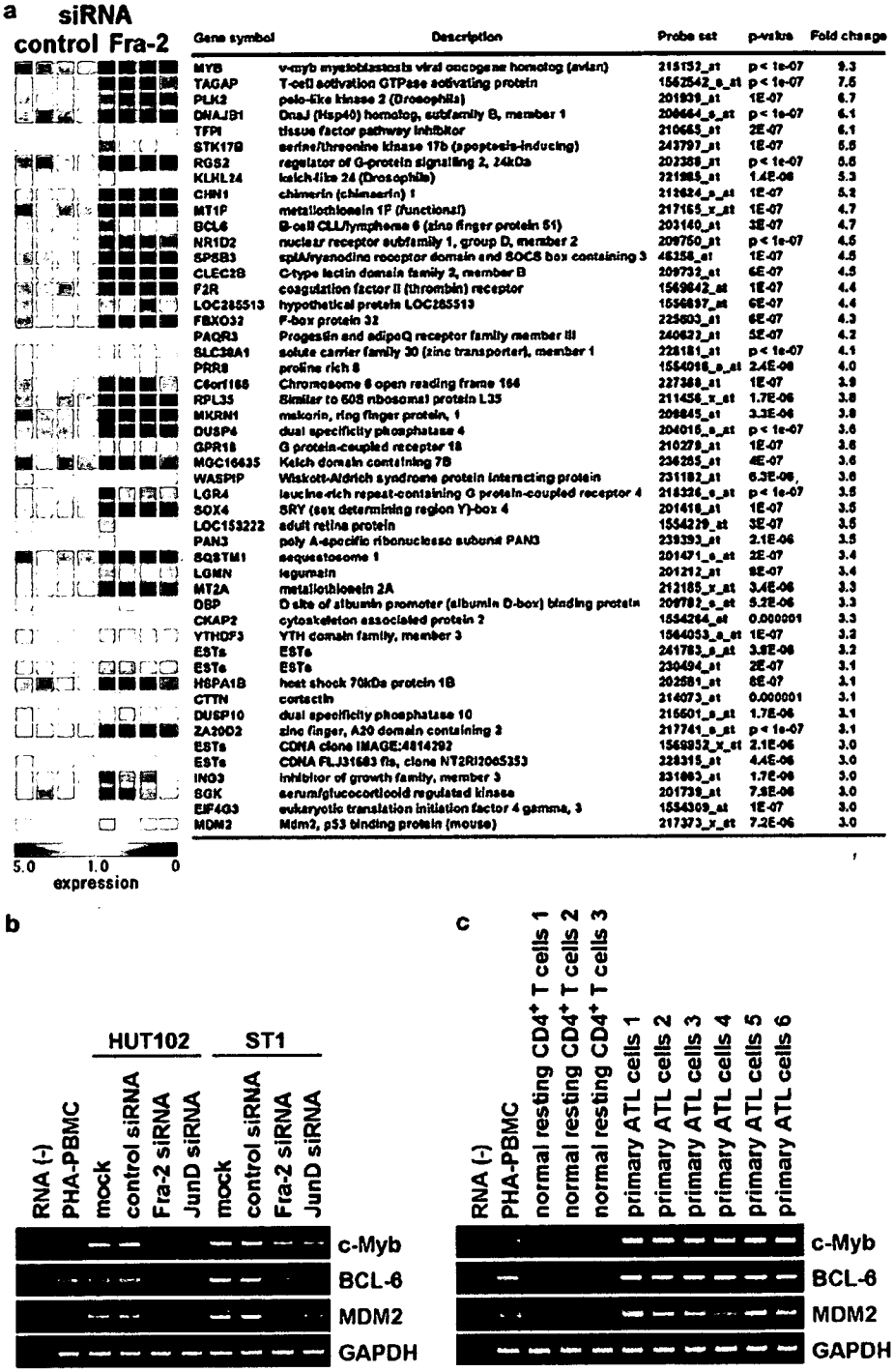

Gene symbol	Description	Probe set	p-value	Fold change
MYB	v-myb myeloblastosis viral oncogene homolog (avian)	215152_at	p< 1e-07	9.3
TAGAP	T-cell activation GTPase activating protein	1562542_a_at	p< 1e-07	7.5
PLK2	polo-like kinase 2 (Drosophila)	201939_at	1E-07	6.7
DNAJB1	DnaJ (Hsp40) homolog, subfamily B, member 1	200664_s_at	p< 1e-07	6.1
TFPI	tissue factor pathway inhibitor	210665_at	2E-07	6.1
STK17B	serine/threonine kinase 17b (apoptosis-inducing)	243797_at	1E-07	5.8
RGS2	regulator of G-protein signalling 2, 24kDa	202388_at	p< 1e-07	5.6
KLHL24	kelch-like 24 (Drosophila)	221985_at	1.4E-06	5.3
CHN1	chimerin (chimaerin) 1	213624_s_at	1E-07	5.2
MT1P	metallothionein 1P (functional)	217165_x_at	1E-07	4.7
BCL6	B-cell CLL/lymphoma 6 (zinc finger protein 51)	203140_at	3E-07	4.7
NR1D2	nuclear receptor subfamily 1, group D, member 2	209750_at	p< 1e-07	4.6
SPSB3	spla/ryanodine receptor domain and SOCS box containing 3	46258_at	1E-07	4.5
CLEC2B	C-type lectin domain family 2, member B	209732_at	6E-07	4.5
F2R	coagulation factor II (thrombin) receptor	1569842_at	1E-07	4.4
LOC285513	hypothetical protein LOC285513	1556897_at	6E-07	4.4
FBXO32	F-box protein 32	225603_at	6E-07	4.3
PAQR3	Progestin and adipoQ receptor family member III	240623_at	5E-07	4.2
SLC39A1	solute carrier family 30 (zinc transporter), member 1	228181_at	p< 1e-07	4.1
PRR8	proline rich 8	1554016_a_at	2.4E-06	4.0
C6orf166	Chromosome 6 open reading frame 166	227368_at	1E-07	3.9
RPL35	Similar to 60S ribosomal protein L35	211456_x_at	1.7E-06	3.8
MKRN1	makorin, ring finger protein, 1	206845_at	3.3E-06	3.8
DUSP4	dual specificity phosphatase 4	204015_s_at	p< 1e-07	3.6
GPR18	G protein-coupled receptor 18	210279_at	1E-07	3.6
MGC16635	Kelch domain containing 7B	236285_at	4E-07	3.6
WASPIP	Wiskott-Aldrich syndrome protein interacting protein	231182_at	6.3E-06	3.6
LGR4	leucine-rich repeat-containing G protein-coupled receptor 4	218326_s_at	p< 1e-07	3.5
SOX4	SRY (sex determining region Y)-box 4	201416_at	1E-07	3.5
LOC153222	adult retina protein	1554229_at	3E-07	3.5
PAN3	poly A-specific ribonuclease subunit PAN3	239393_at	2.1E-06	3.5
SQSTM1	sequestosome 1	201471_s_at	2E-07	3.4
LGMN	legumain	201212_at	8E-07	3.4
MT2A	metallothionein 2A	212185_x_at	3.4E-06	3.3
DBP	D site of albumin promoter (albumin D-box) binding protein	209782_s_at	5.2E-06	3.3
CKAP2	cytoskeleton associated protein 2	1554264_at	0.000001	3.3
YTHDF3	YTH domain family, member 3	1564053_a_at	1E-07	3.2
ESTs	ESTs	241783_s_at	3.8E-06	3.2
ESTs	ESTs	230494_at	2E-07	3.1
HSPA1B	heat shock 70kDa protein 1B	202581_at	8E-07	3.1
CTTN	cortactin	214073_at	0.000001	3.1
DUSP10	dual specificity phosphatase 10	215601_s_at	1.7E-06	3.1
ZA20D2	zinc finger, A20 domain containing 2	217741_s_at	p< 1e-07	3.1
ESTs	CDNA clone IMAGE:4814292	1569852_x_at	2.1E-06	3.0
ESTs	CDNA FLJ31683 fis, clone NT2RI2005353	228315_at	4.4E-06	3.0
ING3	inhibitor of growth family, member 3	231083_at	1.7E-06	3.0
SGK	serum/glucocorticoid regulated kinase	201739_at	7.8E-06	3.0
EIF4G3	eukaryotic translation initiation factor 4 gamma, 3	1554309_at	1E-07	3.0
MDM2	Mdm2, p53 binding protein (mouse)	217373_x_at	7.2E-06	3.0

Figure 6 Identification of downstream target genes of Fra-2 in adult T-cell leukemia (ATL). (a) Microarray analysis. ST1 cells were transfected with control siRNA or Fra-2 siRNA. After 48 h, microarray analysis was performed using the Affymetrix GeneChip HG-U133 Plus 2.0 array. Four independent transfection samples were analysed for each group. Each column represents the expression level of a given gene in an individual sample. Red represents increased expression and blue represents decreased expression relative to the normalized expression of the gene across all samples. We computed the statistical significance level for each gene between the Fra-2-knockdown group and the control group with a mean fold change of > 3 by the *t*-test ($P<10^{-5}$). (b) Reverse transcription (RT)–PCR analysis. HUT102 and ST1 cells were transfected with control siRNA or siRNA for Fra-2 or JunD. After 48 h, the expression of c-Myb, BCL-6, MDM2 and GAPDH was determined by RT–PCR. The representative results from three separate experiments are shown. (c) RT–PCR analysis. Normal $CD4^+$ T cells from healthy donors ($n=3$; purity, > 96%) and PBMC from ATL patients ($n=6$; leukemic cells, > 90%) were examined for the expression of c-Myb, BCL-6 and MDM2 by RT–PCR. The representative results from two separate experiments are shown.

various AP-1 family members in primary ATL cells (patient nos. 1 and 5) and in some ATL cell lines expressing Tax (Figures 2a and b). However, the constitutive expression of Fra-2, JunD and JunB in freshly isolated primary ATL cells and ATL cell lines is apparently independent from Tax expression (Figures 2a and b). This is further supported by the finding that CCR4-expressing HTLV-1-negative CTCL cell lines also constitutively express Fra-2, JunB and JunD at high levels (Figure 2). By using JPX-9, which is a subline of Jurkat carrying the HTLV-1 Tax gene under the control of the metallothionein gene promoter (Nagata *et al.*, 1989), we have also confirmed that Fra-2 is not inducible by Tax (data not shown).

The CCR4 promoter was potently activated by the Fra-2/JunB and Fra-2/JunD heterodimers (Figure 3a). Fra-2, JunB and JunD were also shown to bind specifically to the AP-1 site in the CCR4 promoter *in vitro* by the NoShift binding assays and *in vivo* by the ChIP assays (Figures 4a and b). By using the siRNA knockdown technique, however, only Fra-2 siRNA and JunD siRNA efficiently suppressed CCR4 expression and cell growth in ATL cell lines (Figure 5). On the other hand, JunB siRNA showed little such effect (Figure 5). Therefore, it is likely that, at least in terms of CCR4 expression and cell proliferation, the Fra-2/JunD heterodimer plays a more dominant role than the Fra-2/JunB heterodimer in ATL cells. It thus remains to be determined whether the Fra-2/JunB heterodimer has any specific functions in ATL.

The most striking finding in the present study is the aberrant expression of Fra-2 in primary ATL cells. Fra-2 expression is essentially absent in normal $CD4^+$ T cells under various conditions thus far examined (Figures 2a and c). Physiologically, Fra-2 is known to be expressed by various epithelial cells and in cartilaginous structures and has been shown to be required for efficient cartilage development (Karreth *et al.*, 2004). With regard to lymphoid cells, developing murine thymocytes were reported to express Fra-2 (Chen *et al.*, 1999). Previous studies have shown that individual homodimeric and heterodimeric AP-1 proteins have different functional properties and target genes (Shaulian and Karin, 2002; Eferl and Wagner, 2003). However, little is known about the target genes of Fra-2 and even less is known about the oncogenic role of Fra-2 in human malignancies. In this study, we have shown that CCR4 is the direct target gene of Fra-2 in association with JunD in ATL cells. Furthermore, we have shown that at least 49 genes are downregulated more than threefold in the ATL cell line ST-1 by Fra-2 siRNA (Figure 6). Among these genes, the proto-oncogenes c-Myb, BCL-6 and MDM2 (Oh and Reddy, 1999; Pasqualucci *et al.*, 2003; Vargas *et al.*, 2003) are further confirmed to be dependent on the Fra-2/JunD heterodimer and to be expressed at high levels in primary ATL cells (Figure 6). It remains to be seen whether the Fra-2/JunD heterodimer directly induces these proto-oncogenes or indirectly maintains their expression by promoting cell growth.

c-Myb is the genomic homologue of the avian myeloblastosis virus oncogene v-Myb. c-Myb is widely expressed in immature hematopoietic cells and also in various leukemias and carcinomas (Oh and Reddy, 1999; Shetzline *et al.*, 2004; Hess *et al.*, 2006). The target genes of c-Myb include the anti-apoptotic genes BCL-2 and BCL-X_L and also c-Myc (Ramsay *et al.*, 2003). Thus, c-Myb may promote the survival of ATL cells via BCL-2 and BCL-X_L (Galonek and Hardwick, 2006) and also cell cycle progression via c-Myc (Dang, 1999). BCL-6 was originally identified as the target gene of recurrent chromosomal translocations affecting 3q27 in non-Hodgkin's lymphoma. The expression of BCL-6 is frequently upregulated in diffuse large-cell lymphoma and follicular lymphoma through promoter substitution or somatic promoter point mutations (Ye *et al.*, 1993; Migliazza *et al.*, 1995; Chang *et al.*, 1996). Frequent expression of BCL-6 has also been reported in some T-cell lymphomas (Kerl *et al.*, 2001). The BCL-6 protein has been shown to exert cell-immortalizing and anti-senescence activities (Shvarts *et al.*, 2002; Pasqualucci *et al.*, 2003). Thus, BCL-6 may also inhibit apoptosis and promote cell cycle progression in ATL. The MDM2 protein is a negative regulator of p53 and suppresses p53-mediated cell cycle arrest and apoptosis (Vargas *et al.*, 2003). Elevated expression of MDM2 has been demonstrated in various types of human cancer (Rayburn *et al.*, 2005). Given that only a minor fraction of ATL cases have mutations affecting p53 (Cesarman *et al.*, 1992), the elevated expression of MDM2 may contribute to the functional downregulation of p53 in the majority of ATL cases.

CTCLs are a group of T-cell lymphomas derived from skin-homing memory T cells. CTCLs are not associated with HTLV-1 infection but resemble ATL and frequently express CCR4 (Ferenczi *et al.*, 2002; Kim *et al.*, 2005). Furthermore, CCR4 expression has been shown to be a consistent feature of the large-cell transformation of mycosis fungoides (Jones *et al.*, 2000). In the present study, we have shown that CTCL cell lines also express Fra-2, JunB and JunD at high levels (Figure 2b). Therefore, it is likely that aberrantly expressed Fra-2 in association with Jun proteins, particularly JunD, is also involved in CCR4-expression and cell proliferation in CTCLs.

In conclusion, we have shown that aberrantly expressed Fra-2 in association with JunD is responsible for CCR4 expression in ATL and is also likely to play an important role in ATL oncogenesis in part by inducing the expression of the proto-oncogenes c-Myb, BCL-6 and MDM2. Future studies are necessary to elucidate how the Fra-2/JunD heterodimer induces the expression of these proto-oncogenes and their individual roles in ATL oncogenesis. It also remains to be seen how ATL cells aberrantly express Fra-2 at high levels. Furthermore, the expression and function of Fra-2 in CTCLs remain to be determined.

Materials and methods

Cells

All the human T-cell lines used were described previously (Nagata *et al.*, 1989; Yamada *et al.*, 1996; Hata *et al.*, 1999;

Yoshie *et al.*, 2002). Peripheral blood mononuclear cells (PBMC) were isolated from heparinized blood samples obtained from healthy adult donors and acute ATL patients with a high leukemic cell count (>90%) by using Ficoll-Paque (Amersham Biosciences Corp, Piscataway, NJ, USA). Normal $CD4^+$ T cells (purity, >96%) were further prepared from PBMC by negative selection using an IMagnet system (BD Pharmingen, San Diego, CA, USA). Activated $CD4^+$ T cells were prepared by stimulating $CD4^+$ T cells with anti-CD3 (clone HIT3a; BD Pharmingen) and anti-CD28 (clone CD28.2; BD Pharmingen) for 24 h. The preparation of naive $CD4^+CD45RA^+$ T cells and their polarization into Th1 and Th2 cells were performed as described previously (Imai *et al.*, 1999). Primary ATL cells and normal resting $CD4^+$ T cells were used without culture for the experiments. This study was approved by the local ethical committee and written informed consent was obtained from each patient.

Transfection and luciferase assay

The major transcriptional start site (+1) of the human CCR4 gene was determined by the method of rapid amplification of cDNA 5′-ends and was found to be located 1797 bases upstream from the translation start codon (data not shown). To generate a promoter–reporter construct, the 1-kb promoter region of the human CCR4 gene (−983 to +25) was amplified from the genomic DNA by PCR using primers based on a GenBank genomic DNA sequence (accession no. NC_000003) and inserted into the reporter plasmid pGL3-Basic (Promega, Madison, WI, USA). Deletions and site-directed mutations were also performed using PCR. pGL3-2xAP-1 was constructed by introducing a sequence containing two copies of the AP-1 consensus binding site (TGATGACTCAGCCGGAATGATGACTCAGCC) in front of a minimal CCR4 promoter pGL3 (−96/+25; Figure 1b). The coding regions of human FosB and GATA-3 were amplified from a cDNA library generated from phytohemagglutinin (PHA)-stimulated PBMC by PCR and cloned into the expression vector pSG5 (Stratagene, La Jolla, CA, USA). The coding region of HTLV-1 HBZ was amplified from a cDNA library generated from the HTLV-1^+ T-cell line C8166 by PCR and cloned into the expression vector pEF4/myc-His A (Invitrogen, Carlsbad, CA, USA). The expression vectors for c-Fos, Fra-1, Fra-2, c-Jun, JunB, JunD and Tax were described previously (Iwai *et al.*, 2001). Cells (5×10^5) were transfected with 2 μg of reporter plasmid, 0.5 μg of expression plasmids for various transcription factors and 1 μg of pSV-β-galactosidase using DMRIE-C (Invitrogen). After 24–27 h, luciferase assays were performed using a Luciferase Assay kit (Promega). Luciferase activity was normalized by β-galactosidase activity that served as an internal control for transfection efficiency.

RT–PCR

RT–PCR was carried out as described previously (Yoshie *et al.*, 2002). The primers used were as follows: +5′-AAGAAGAACAAGGCGGTGAAGATG-3′ and −5′-AGGCCCCTGCAGGTTTTGAAG-3′ for CCR4; +5′-TACTACCACTCACCCGCAGACTC-3′ and −5′-CTTTTCCCTTCGGATTCTCCTTTT-3′ for c-Fos; +5′-TAGCAGCAGCTAAATGCAGGAAC-3′ and −5′-CCAGCTGAAGCCATCTTCCTTAG-3′ for FosB; +5′-CAGTGGATGGTACAGCCTCATTT-3′ and −5′-GCCCAGATTTCTCATCTTCCAGT-3′ for Fra-1; +5′-CCAGCAGAAATTCCGGGTAGATA-3′ and −5′-TCTCCTCCTCTTCAGGAGACAGC-3′ for Fra-2; +5′-AAACAGAGCATGACCCTGAACCT-3′ and −5′-CTCCTGCTCATCTGTCACGTTCT-3′ for c-Jun; +5′-AAAATGGAACAGCCCTTCTACCA-3′ and −5′-AGCCCTGACCAGAAAAGTAGCTG-3′ for JunB; +5′-AACACCCTTCTACGGCGATGAG-3′ and −5′-GGGTAGAGGAACTGTGAGCTCGT-3′ for JunD; +5′-GAATTGGTGGACGGGCTATTATC-3′ and −5′-TAGCACTATGCTGTTTCGCCTTC-3′ for HBZ; +5′-CCGGCGCTGCTCTCATCCCGGT-3′ and −5′-GGCCGAACATAGTCCCCCAGAG-3′ for Tax; +5′-AAGGCATCCAGACCAGAAACCG-3′ and −5′-AGCATCGAGCAGGGCTCTAACC-3′ for GATA-3; +5′-CAGTGACGAGGATGATGAGGACT-3′ and −5′-AACGTTTCGGACCGTATTTCTGT-3′ for c-Myb; +5′-ATTCCAGCTTCGGAACAAGAGAC-3′ and −5′-GTCCTTTTGATCACTCCCACCTT-3′ for MDM2; +5′-CAAGAAGTTTCTAGGAAAGGCCGG-3′ and −5′-GATTGATCACACTAAGGTTGCATT-3′ for BCL-6 and +5′-GCCAAGGTCATCCATGACAACTTTGG-3′ and −5′-GCCTGCTTCACCACCTTCTTGATGTC-3′ for glyceraldehyde-3-phosphate dehydrogenase (GAPDH). The amplification conditions were denaturation at 94 °C for 30 s (5 min for the first cycle), annealing at 60 °C for 30 s and extension at 72 °C for 30 s (5 min for the last cycle) for 34 cycles for CCR4; 35 cycles for c-Fos, FosB, Fra-1, Fra-2, c-Jun, JunB, JunD, HBZ, Tax, c-Myb, BCL-6 and MDM2; 29 cycles for GATA-3 and 27 cycles for GAPDH. Amplification products were electrophoretically run on a 2% agarose gel and stained with ethidium bromide.

Quantitative real-time PCR was carried out using the TaqMan assay and a 7700 Sequence Detection System (Applied Biosystems, Foster City, CA, USA). The conditions for PCR were 50 °C for 2 min, 95 °C for 10 min and then 50 cycles of 95 °C for 15 s (denaturation) and 60 °C for 1 min (annealing extension). The primers and fluorogenic probes for CCR4 and 18S ribosomal RNA were obtained from a TaqMan kit (Applied Biosystems). Quantification of CCR4 expression was performed using the Sequence Detector System Software (Applied Biosystems).

NoShift transcription factor assay

Anti-c-Fos (sc-52), anti-FosB (sc-7203), anti-Fra-1 (sc-22794), anti-Fra-2 (sc-604), anti-c-Jun (sc-1694), anti-JunB (sc-73) and anti-JunD (sc-74) were purchased from Santa Cruz Biotechnology (Santa Cruz, CA, USA). Transcription factors bound to specific DNA sequences were identified using the NoShift Transcription Factor Assay Kit (EMD Biosciences, Madison, WI, USA). Nuclear extracts were prepared from human T-cell lines by using the NucBuster Protein Extraction Kit (EMD Biosciences). The oligonucleotides used were as follows (differences underlined): TGGGAAATGACTAAGAATCAT for the biotinylated probe and unlabeled competitor of the AP-1 site and TGGGAAATGTCAAAGAATCAT for the mutated AP-1 site.

ChIP assay

This assay was performed using a ChIP assay kit (Upstate Biotechnology, Lake Placid, NY, USA) following the manufacturer's instructions. In brief, cells (1×10^6) were cross-linked with 1% formaldehyde for 10 min at room temperature. The cell pellets were lysed with sodium dodecyl sulfate (SDS) lysis buffer and sonicated to shear DNA to a size range between 200 and 1000 bp. After centrifugation, the supernatant was diluted 10-fold in ChIP dilution buffer and incubated overnight at 4 °C with 4 μg of anti-Fra-2 (sc-604), anti-JunB (sc-73), anti-JunD (sc-74) or normal rabbit IgG (DAKO, Kyoto, Japan). Immunocomplexes were collected by adding protein A-agarose beads. The immune complexes were incubated at 65 °C for 4 h to reverse the protein/DNA cross-links. DNAs were then purified by phenol/chloroform extraction and used as templates for quantitative real-time PCR. The primers and

the fluorogenic probe for the AP-1 site of the CCR4 promoter were as follows: primers: +5′-GGTCTTGGGAAATGACT AAGAATCA-3′ and −5′-TCTCCCTCACCCAACTGTACT AAGT-3′; probe: 5′-TCTGCTTCCTACTTCTATCAAA AAACCCCACTTG-3′.

Immunological staining
Cells were spotted on a glass slide and fixed with 4% paraformaldehyde. Tissue sections were prepared from formalin-fixed and paraffin-embedded biopsy tissue samples and subjected to microwave irradiation for 5 min three times in Target Retrieval Solution (DAKO). Slides and tissue sections were incubated for 1 h at room temperature with anti-Fra-2 (sc-604), anti-JunB (sc-73), anti-JunD (sc-74) or mouse monoclonal anti-CCR4 (KM-2160; Kyowa Hakko, Tokyo, Japan). Normal rabbit IgG and control mouse IgG_1 (DAKO) were used as negative controls. After washing, the slides and tissue sections were incubated with biotin-labeled goat anti-rabbit IgG or biotin-labeled horse anti-mouse IgG followed by detection using the Vectastain ABC/HRP kit (Vector Laboratories, Burlingame, CA, USA). Finally, cells and sections were counterstained with Gill's hematoxylin (Polysciences, Warrington, PA, USA), dehydrated and mounted.

Transfection of siRNA
siRNAs for Fra-2 (SI00420455), JunB (SI03077445), JunD (SI00075985) and the negative control (1022064) were obtained from Qiagen (Hilden, Germany). Transfection experiments were performed using Amaxa Nucleofector (Amaxa, Cologne, Germany). Cells (1×10^6) were resuspended in 100 µl of Nucleofector solution (T solution for MOLT-4, HUT102 and ST1 and V solution for Jurkat) and transfected with 2.5 µg of siRNA using program O-17 for MOLT-4, HUT102 and ST1 and program S-18 for Jurkat. The transfection efficiency was ~95% as determined using fluorescent siRNA (Qiagen).

Cell proliferation assay
Cells were seeded in a 96-well plate at a density of 0.5×10^4 per well and cultured. The number of viable cells was determined every 24 h on a FACSCalibur system (Becton Dickinson, Mountain View, CA, USA) by gating out cells stained with propidium iodide. To prepare stable transfectants of Fra-2 and JunD, the coding regions of human Fra-2 and JunD were inserted into the pIRES2-EGFP vector (BD Biosciences, San Diego, CA, USA). Jurkat cells were transfected with the plasmids using DMRIE-C (Invitrogen). Stable transfectants expressing green fluorescence protein were sorted by flow cytometry using FACSVantage (Becton Dickinson).

Oligonucleotide microarray
Microarray analysis was performed as described previously (Igarashi *et al.*, 2007) using the Affymetrix GeneChip HG-U133 Plus 2.0 array (Affymetrix, Santa Clara, CA, USA). In brief, the ATL-derived cell line ST1 was transfected with control siRNA or Fra-2 siRNA. Four independent transfections were performed for each group. After 48 h, total RNA samples were prepared and confirmed to be of good quality with the Agilent 2100 Bioanalyzer (Agilent Technologies, Waldbronn, Germany). All microarray data have been submitted to the Gene Expression Omnibus (GEO; http://www.ncbi.nlm.nih.gov/geo; accession no. GSE6379). The analysis was performed using the BRB Array Tools software version 3.3.0 (http://linus.nci.nih.gov/BRB-ArrayTools.html) developed by Richard Simon and Amy Peng.

Acknowledgements

We thank Namie Sakiyama for her excellent technical assistance. We also thank Dr Rich Simon and Dr Amy Peng for providing the BRB ArrayTools software. This work was supported in part by a Grant-in-Aid from the Ministry of Education, Culture, Sports and Technology, Japan; by Solution-Oriented Research for Science and Technology (SORST) from Japan Science and Technology Corporation and by High-Tech Research Center Project for Private Universities: matching fund subsidy from the Ministry of Education, Culture, Sports, Science and Technology of Japan, 2002–2009.

References

Basbous J, Arpin C, Gaudray G, Piechaczyk M, Devaux C, Mesnard JM. (2003). The HBZ factor of human T-cell leukemia virus type I dimerizes with transcription factors JunB and c-Jun and modulates their transcriptional activity. *J Biol Chem* **278**: 43620–43627.

Cesarman E, Chadburn A, Inghirami G, Gaidano G, Knowles DM. (1992). Structural and functional analysis of oncogenes and tumor suppressor genes in adult T-cell leukemia/lymphoma shows frequent p53 mutations. *Blood* **80**: 3205–3216.

Chang CC, Ye BH, Chaganti RS, Dalla-Favera R. (1996). BCL-6, a POZ/zinc-finger protein, is a sequence-specific transcriptional repressor. *Proc Natl Acad Sci USA* **93**: 6947–6952.

Chen F, Chen D, Rothenberg EV. (1999). Specific regulation of fos family transcription factors in thymocytes at two developmental checkpoints. *Int Immunol* **11**: 677–688.

Dang CV. (1999). c-Myc target genes involved in cell growth, apoptosis, and metabolism. *Mol Cell Biol* **19**: 1–11.

Eferl R, Wagner EF. (2003). AP-1: a double-edged sword in tumorigenesis. *Nat Rev Cancer* **3**: 859–868.

Ferenczi K, Fuhlbrigge RC, Pinkus J, Pinkus GS, Kupper TS. (2002). Increased CCR4 expression in cutaneous T cell lymphoma. *J Invest Dermatol* **119**: 1405–1410.

Galonek HL, Hardwick JM. (2006). Upgrading the BCL-2 Network. *Nat Cell Biol* **8**: 1317–1319.

Grassmann R, Aboud M, Jeang KT. (2005). Molecular mechanisms of cellular transformation by HTLV-1 Tax. *Oncogene* **24**: 5976–5985.

Hata T, Fujimoto T, Tsushima H, Murata K, Tsukasaki K, Atogami S *et al.* (1999). Multi-clonal expansion of unique human T-lymphotropic virus type-I-infected T cells with high growth potential in response to interleukin-2 in prodromal phase of adult T cell leukemia. *Leukemia* **13**: 215–221.

Hess JL, Bittner CB, Zeisig DT, Bach C, Fuchs U, Borkhardt A *et al.* (2006). c-Myb is an essential downstream target for homeobox-mediated transformation of hematopoietic cells. *Blood* **108**: 297–304.

Hori S, Nomura T, Sakaguchi S. (2003). Control of regulatory T cell development by the transcription factor Foxp3. *Science* **299**: 1057–1061.

Iellem A, Mariani M, Lang R, Recalde H, Panina-Bordignon P, Sinigaglia F *et al.* (2001). Unique chemotactic response profile and specific expression of chemokine receptors CCR4 and CCR8 by CD4(+)CD25(+) regulatory T cells. *J Exp Med* **194**: 847–853.

Igarashi T, Izumi H, Uchiumi T, Nishio K, Arao T, Tanabe M *et al.* (2007). Clock and ATF4 transcription system regulates drug resistance in human cancer cell lines. *Oncogene* **26**: 4749–4760.

Imai T, Nagira M, Takagi S, Kakizaki M, Nishimura M, Wang J *et al.* (1999). Selective recruitment of CCR4-bearing Th2 cells toward antigen-presenting cells by the CC chemokines thymus and

activation-regulated chemokine and macrophage-derived chemokine. *Int Immunol* **11**: 81–88.

Ishida T, Utsunomiya A, Iida S, Inagaki H, Takatsuka Y, Kusumoto S *et al.* (2003). Clinical significance of CCR4 expression in adult T-cell leukemia/lymphoma: its close association with skin involvement and unfavorable outcome. *Clin Cancer Res* **9**: 3625–3634.

Iwai K, Mori N, Oie M, Yamamoto N, Fujii M. (2001). Human T-cell leukemia virus type 1 tax protein activates transcription through AP-1 site by inducing DNA binding activity in T cells. *Virology* **279**: 38–46.

Jeang KT, Chiu R, Santos E, Kim SJ. (1991). Induction of the HTLV-I LTR by Jun occurs through the Tax-responsive 21-bp elements. *Virology* **181**: 218–227.

Jones D, O C, Kraus MD, Perez-Atayde AR, Shahsafaei A, Wu L *et al.* (2000). Expression pattern of T-cell-associated chemokine receptors and their chemokines correlates with specific subtypes of T-cell non-Hodgkin lymphoma. *Blood* **96**: 685–690.

Karreth F, Hoebertz A, Scheuch H, Eferl R, Wagner EF. (2004). The AP1 transcription factor Fra2 is required for efficient cartilage development. *Development* **131**: 5717–5725.

Karube K, Ohshima K, Tsuchiya T, Yamaguchi T, Kawano R, Suzumiya J *et al.* (2004). Expression of FoxP3, a key molecule in CD4CD25 regulatory T cells, in adult T-cell leukaemia/lymphoma cells. *Br J Haematol* **126**: 81–84.

Kerl K, Vonlanthen R, Nagy M, Bolzonello NJ, Gindre P, Hurwitz N *et al.* (2001). Alterations on the 5′ noncoding region of the BCL-6 gene are not correlated with BCL-6 protein expression in T cell non-Hodgkin lymphomas. *Lab Invest* **81**: 1693–1702.

Kim EJ, Hess S, Richardson SK, Newton S, Showe LC, Benoit BM *et al.* (2005). Immunopathogenesis and therapy of cutaneous T cell lymphoma. *J Clin Invest* **115**: 798–812.

Matsubara Y, Hori T, Morita R, Sakaguchi S, Uchiyama T. (2005). Phenotypic and functional relationship between adult T-cell leukemia cells and regulatory T cells. *Leukemia* **19**: 482–483.

Matsuoka M. (2003). Human T-cell leukemia virus type I and adult T-cell leukemia. *Oncogene* **22**: 5131–5140.

Migliazza A, Martinotti S, Chen W, Fusco C, Ye BH, Knowles DM *et al.* (1995). Frequent somatic hypermutation of the 5′ noncoding region of the BCL6 gene in B-cell lymphoma. *Proc Natl Acad Sci USA* **92**: 12520–12524.

Mori N, Fujii M, Ikeda S, Yamada Y, Tomonaga M, Ballard DW *et al.* (1999). Constitutive activation of NF-kappaB in primary adult T-cell leukemia cells. *Blood* **93**: 2360–2368.

Mori N, Fujii M, Iwai K, Ikeda S, Yamasaki Y, Hata T *et al.* (2000). Constitutive activation of transcription factor AP-1 in primary adult T-cell leukemia cells. *Blood* **95**: 3915–3921.

Nagakubo D, Jin Z, Hieshima K, Nakayama T, Shirakawa AK, Tanaka Y *et al.* (2007). Expression of CCR9 in HTLV-1$^+$ T cells and ATL cells expressing Tax. *Int J Cancer* **120**: 1591–1597.

Nagata K, Ohtani K, Nakamura M, Sugamura K. (1989). Activation of endogenous c-fos proto-oncogene expression by human T-cell leukemia virus type I-encoded p40tax protein in the human T-cell line, Jurkat. *J Virol* **63**: 3220–3226.

Oh IH, Reddy EP. (1999). The myb gene family in cell growth, differentiation and apoptosis. *Oncogene* **18**: 3017–3033.

Pasqualucci L, Bereschenko O, Niu H, Klein U, Basso K, Guglielmino R *et al.* (2003). Molecular pathogenesis of non-Hodgkin's lymphoma: the role of Bcl-6. *Leuk Lymphoma* **44**(Suppl 3): S5–S12.

Ramsay RG, Barton AL, Gonda TJ. (2003). Targeting c-Myb expression in human disease. *Expert Opin Ther Targets* **7**: 235–248.

Rayburn E, Zhang R, He J, Wang H. (2005). MDM2 and human malignancies: expression, clinical pathology, prognostic markers, and implications for chemotherapy. *Curr Cancer Drug Targets* **5**: 27–41.

Rengarajan J, Szabo SJ, Glimcher LH. (2000). Transcriptional regulation of Th1/Th2 polarization. *Immunol Today* **21**: 479–483.

Satou Y, Yasunaga J, Yoshida M, Matsuoka M. (2006). HTLV-I basic leucine zipper factor gene mRNA supports proliferation of adult T cell leukemia cells. *Proc Natl Acad Sci USA* **103**: 720–725.

Shaulian E, Karin M. (2002). AP-1 as a regulator of cell life and death. *Nat Cell Biol* **4**: E131–E136.

Shetzline SE, Rallapalli R, Dowd KJ, Zou S, Nakata Y, Swider CR *et al.* (2004). Neuromedin U: a Myb-regulated autocrine growth factor for human myeloid leukemias. *Blood* **104**: 1833–1840.

Shvarts A, Brummelkamp TR, Scheeren F, Koh E, Daley GQ, Spits H *et al.* (2002). A senescence rescue screen identifies BCL6 as an inhibitor of anti-proliferative p19(ARF)-p53 signaling. *Genes Dev* **16**: 681–686.

Thebault S, Basbous J, Hivin P, Devaux C, Mesnard JM. (2004). HBZ interacts with JunD and stimulates its transcriptional activity. *FEBS Lett* **562**: 165–170.

Vargas DA, Takahashi S, Ronai Z. (2003). Mdm2: a regulator of cell growth and death. *Adv Cancer Res* **89**: 1–34.

Yamada Y, Ohmoto Y, Hata T, Yamamura M, Murata K, Tsukasaki K *et al.* (1996). Features of the cytokines secreted by adult T cell leukemia (ATL) cells. *Leuk Lymphoma* **21**: 443–447.

Yamamoto N, Hinuma Y. (1985). Viral aetiology of adult T-cell leukaemia. *J Gen Virol* **66**: 1641–1660.

Ye BH, Lista F, Lo Coco F, Knowles DM, Offit K, Chaganti RS *et al.* (1993). Alterations of a zinc finger-encoding gene, BCL-6, in diffuse large-cell lymphoma. *Science* **262**: 747–750.

Yoshida M. (2001). Multiple viral strategies of HTLV-1 for dysregulation of cell growth control. *Annu Rev Immunol* **19**: 475–496.

Yoshie O, Fujisawa R, Nakayama T, Harasawa H, Tago H, Izawa D *et al.* (2002). Frequent expression of CCR4 in adult T-cell leukemia and human T-cell leukemia virus type 1-transformed T cells. *Blood* **99**: 1505–1511.

Yoshie O, Imai T, Nomiyama H. (2001). Chemokines in immunity. *Adv Immunol* **78**: 57–110.

Lung Cancer (2007) 57, 302–310

available at www.sciencedirect.com

ScienceDirect

journal homepage: www.elsevier.com/locate/lungcan

LUNG CANCER

Abrogation of the interaction between osteopontin and αvβ3 integrin reduces tumor growth of human lung cancer cells in mice

Ri Cui[a,b,*], Fumiyuki Takahashi[a,b], Rina Ohashi[a,b], Tao Gu[a,b], Masakata Yoshioka[a,b], Kazuto Nishio[c], Yuichiro Ohe[d], Shigeru Tominaga[a], Yumiko Takagi[a,b], Shinichi Sasaki[a], Yoshinosuke Fukuchi[a,b], Kazuhisa Takahashi[a,b]

[a] *Department of Respiratory Medicine and Research Institute for Diseases of Old Ages, Juntendo University, School of Medicine, 2-1-1 Hongo, Bunkyo-Ku, Tokyo 113-8421, Japan*
[b] *Research Institute for Diseases of Old Ages, Juntendo University, School of Medicine, 2-1-1 Hongo, Bunkyo-Ku, Tokyo 113-8421, Japan*
[c] *Pharmacology Division, National Cancer Center Research Institute, 5-1-1 Tsukiji, Chuo-Ku, Tokyo 104-0045, Japan*
[d] *Department of Internal Medicine, National Cancer Center Hospital, 5-1-1 Tsukiji, Chuo-Ku, Tokyo 104-0045, Japan*

Received 4 January 2007; received in revised form 15 March 2007; accepted 18 March 2007

KEYWORDS
Osteopontin;
Angiogenesis;
αvβ3 integrin;
Tumor growth;
Lung cancer

Summary Osteopontin (OPN) is a multifunctional cytokine involved in cell signaling by interacting with αvβ3 integrins. Recent clinical studies have indicated that OPN expression is associated with tumor progression and poor prognosis among patients with lung cancer. However, the biological role of OPN in human lung cancer has not yet been well-defined. The purpose of this study is to investigate and provide evidence for the causal role of OPN regarding tumor growth and angiogenesis in human lung cancer. In this study, we developed a stable OPN transfectant from human lung cancer cell line SBC-3 which does not express the intrinsic OPN mRNA. To reveal the in vivo effect of OPN on tumor growth of human lung cancer, we subcutaneously injected OPN-overexpressing SBC-3 cells (SBC-3/OPN) and control cells (SBC-3/NEO) into the nude mice. Transfection with the OPN gene significantly increased in vivo tumor growth and neovascularization of SBC-3 cells in mice. These in vivo effects of OPN were markedly suppressed with administration of anti-αvβ3 integrin monoclonal antibody or anti-angiogenic agent, TNP-470. Furthermore, recombinant OPN protein enhanced human umbilical vein endothelial cell (HUVEC) proliferation in vitro, and this enhancement was significantly inhibited with the

* Corresponding author at: Department of Respiratory Medicine, Juntendo University, School of Medicine, 2-1-1 Hongo, Bunkyo-Ku, Tokyo 113-8421, Japan. Tel.: +81 3 5802 1063; fax: +81 3 5802 1617.
E-mail address: cri@med.juntendo.ac.jp (R. Cui).

0169-5002/$ – see front matter
doi:10.1016/j.lungcan.2007.03.019

addition of anti-αvβ3 integrin antibody. Taken together, these results suggest that OPN plays a crucial role for tumor growth and angiogenesis of human lung cancer cells in vivo by interacting with αvβ3 integrin. Targeting the interaction between OPN and αvβ3 integrin could be effective for future development of anti-angiogenic therapeutic agents for patients with lung cancer.

1. Introduction

Lung cancer is one of the most frequently diagnosed solid tumors in the world, and is the leading cause of cancer-related deaths in Japan [1]. Despite advancement and improvements in surgical and medical treatments, the prognosis of lung cancer patients remains extremely poor [2]. These facts indicate how important it is to identify novel target molecules for the development of new anticancer therapies for human lung cancer.

Tumor growth and metastasis depend on blood supply and vessel formation. Therefore, anti-angiogenic therapy appears to be an attractive and rational approach for the treatment of solid tumors including lung cancer [3,4]. One approach to anti-angiogenic therapy is to inhibit the adhesive interactions required for tumor angiogenesis. The migration and proliferation of vascular endothelial cells is dependent on their adhesiveness to extracellular matrix (ECM) proteins through a variety of cell adhesion receptor including αvβ3 integrin [5,6]. Thus, the interaction between ECM and αvβ3 integrin may be a therapeutic target for lung cancer patients.

Osteopontin (OPN) is a multifunctional phosphoprotein that binds to αv integrin at the arginine-glycine-asparatic acid (RGD) motif of the central portion and exerts cell-adhesion and migration activity [7,8]. OPN is one of the ECM proteins produced by cancer cells, and is revealed to be overexpressed in various human tumors including the lung, breast, colon, ovary, and gastric cancers [9–14]. Previous studies suggested that OPN may be involved in the angiogenesis of cancer cells. For example, Senger et al. reported that OPN promotes vascular endothelial cell migration via αv integrin in cooperation with vascular endothelial growth factor (VEGF), suggesting that OPN may be involved in angiogenesis [15]. Shijubo et al. demonstrated that coexpression of OPN and VEGF is closely associated with angiogenesis and poor prognosis in stage I lung adenocarcinoma [16]. Thus, OPN is postulated to be related with tumor progression and angiogenesis in various cancers.

Recently, much interest has been focused on OPN expression in human lung cancer. Donati et al. investigated on the correlation between OPN expression in tumor tissues and survival of 136 patients with stage I non-small cell lung cancer (NSCLC), and indicated that OPN expression is a significant unfavorable prognostic factor for survival among patients with stage I NSCLC [17]. Hu et al. also reported that OPN expression was associated with tumor growth, tumor staging, and lymph node invasion of patients with NSCLC. They further analyzed OPN levels in plasma, and suggest that plasma OPN levels may serve as a biomarker for diagnosing or monitoring patients with NSCLC [18]. These findings from these clinical studies imply that OPN may be a therapeutic target and useful biomarker for human lung cancer. However, the biological and functional role of OPN in lung cancer animal model and therapeutic trials targeting OPN and its receptor, αvβ3 integrin, have not yet been reported.

In this study, we first developed stable transfectants from human small cell lung cancer (SCLC) cell line SBC-3 that constitutively secrete mouse OPN. We demonstrated that OPN transfected SBC-3 cells significantly increased in vivo tumorigenecity and neovascularization in comparison with the control cells in mice. In addition, we evaluated the therapeutic efficacy of anti-mouse αvβ3 integrin antibody (RMV-7) against OPN-overexpressing SBC-3 cells inoculated mice. The biological significance of OPN in tumor growth and angiogenesis of lung cancer and potential treatment using RMV-7 antibody are also discussed.

2. Materials and methods

2.1. Cell lines and reagents

Human small cell lung cancer cell line, SBC-3 cells, was kindly provided by Dr. I. Kimura (Okayama University, Okayama), and cultured in RPMI1640 (Koujin Bio, Saitama, Japan) medium containing 10% (v/v) fetal calf serum. HUVEC were purchased from Clonetics (San Diego, CA) and maintained with EGM-2 medium (Clonetics) on collagen-coated plastic flasks. The anti-mouse αvβ3 antibody (RMV-7) was kindly provided by Prof. Okumura (Department of Immunology, Juntendo University), and has been proven to interfere with OPN-mediated cell migration, adhesion, and proliferation [19,20]. Anti-human αvβ3 monoclonal antibody (LM609) was purchased from Chemicon International (Australia). The monoclonal antibody against murine CD31 was purchased from Phamingen (San Diego, CA). The monoclonal antibody against murine OPN was purchased from Immuno-Biological Laboratories (Gunma, Japan). The polyclonal rabbit anti-single stranded DNA (ssDNA) was purchased from Dakocytomation (Tokyo, Japan). TNP-470 (6-*O*-(*N*-chloroacethyl-carbamoyl)-fumagillol), a semisynthetic analog of fumagillin derived from *Aspergillus fumigatus*, was kindly provided by Takeda Chemical Industries (Osaka, Japan).

2.2. Transfection

5×10^5 SBC-3 cells were transfected with Lipofectamine Reagent (Invitrogen) using 8 μg of purified murine OPN cDNA cloned into the eukaryotic cDNA expression vector BMGneo as previously described [21]. This plasmid was designated as BMGneo-mOPN. Two days later, the cells were placed in G418 sulfate (Geneticin; Invitrogen) at 1 mg/ml for selection. Four weeks after transfection, G418-resistant colonies were expanded and isolated with limiting dilution. The

resulting selected and isolated SBC-3 cells transfected with BMGneo-mOPN and BMGneo were designated as SBC-3/OPN and SBC-3/NEO, respectively.

2.3. Detection of OPN and VEGF transcription by RT-PCR

Expression of OPN and VEGF mRNA were assessed by RT-PCR. Total RNAs were extracted from cultured cell lines with TRIzol reagent (Invitrogen). The primers for the RT-PCR were: OPN sense primer (5′-AGTCGACATGAGATTGGCAGTGATTTGC-3′), OPN anti-sense primer (5′-ACTCGAGGCCTCTTCTTTAGTTGACCTC-3′), VEGF sense primer (5′-TGCACCCATGGCAGAAGGAGG-3′), and VEGF anti-sense primer (5′-TCACCGCCTCGGCTTGTCACA-3′). RT-PCR was conducted using a Gene Amp RNA PCR kit (Applied Biosystems, Branchburg, NJ) according to the manufacture's instructions.

2.4. Determination of OPN protein secretion by ELISA

5×10^5 SBC-3/OPN transfectants were cultured in 6-well plates with 2% FCS in RPMI 1640 medium overnight, followed by incubation in 3 ml serum free medium for an additional 24 h. Secreted murine OPN protein level in culture supernatant was measured with the commercial ELISA kit (Immuno-Biological Laboratories, Gunma, Japan) according to the manufacturer's instruction.

2.5. Western blot analysis

Conditioned medium from SBC-3/OPN and SBC-3/NEO cells were subjected to western blot analysis. Samples were separated on 10% acrylamide gels and transferred to a nitrocellulose filter with electroblotting at 4 °C. The filters were blocked in phosphate-buffered saline (PBS) containing 10% dry milk, washed in PBS containing 1% dry milk and 0.5% Tween-20, and then incubated with polyclonal rabbit anti-mouse OPN antibody (Immuno-Biological Laboratories, Gunma, Japan) at room temperature for 1 h. Filters were again washed and then incubated with horseradish-peroxidase-conjugated anti-rabbit antibody (Amersham Pharmacia Biotech) for 1 h. Filters were then washed with TBST (150 mM NaCl, 10 mM Tris, pH 8.0, 0.05% Tween-20), and specific proteins were detected using the enhanced chemiluminescence system (Amersham Pharmacia Biotech).

2.6. In vitro cell growth rates

SBC-3/NEO and SBC-3/OPN were placed onto 96-well plates at 2×10^3 cells/well in triplicate. At designated time points, the number of cells were quantified using a colormetric MTT assay as described previously [22].

2.7. In vitro cell migration assay

SBC-3/OPN and SBC-3/NEO were transfered to 6-well culture plates at 5×10^5 cells/well and incubated with 2% FCS in RPMI 1640 medium overnight. The cells were washed in PBS, and 3 ml of serum free medium were added to each well. After 24 h, 3 ml of conditioned serum-free medium were collected and subjected to in vitro cell migration assay. In vitro cell migration was performed using a cell culture insert with 8 μm micropore membrane (Falcon; Becton Dickinson, Franklin Lake, NJ) as previously described [21]. Briefly, the suspension of HUVEC (5×10^4 cells/200 μl in RPMI 1640 containing 0.1% BSA) was added to the upper chamber and the collected medium was added to the lower chamber. In order to confirm cell migration mediated by OPN, we conducted additional experiments by treating the cells with GRGDS peptide (Sigma) at the concentration of 100 μM or anti-human αvβ3 antibody at the concentration of 10 μg/ml. After incubation at 37 °C for 8 h, the filters were fixed with 10% formalin, and stained with crystal violet. The cells on the upper surface of the filters were removed by swabbing with a cotton swab, and the cells that had migrated to the lower surface were counted under a microscope at the magnification of 200×. All assays were performed in triplicate and at least three independent experiments were performed.

2.8. Soft agar colony formation assay

Six-well culture plates were covered with a layer of 0.5% agar in RPMI 1640 medium containing 20% (v/v) fetal calf serum to prevent the attachment of the cells to plastic substratum. Cell suspensions (5×10^3 cells/well) of the SBC-3/OPN or SBC-3/NEO cells were prepared with 0.3% agar and poured into 6-well plates. After 2 weeks of incubation at 37 °C, the colonies containing at least 50 cells were counted. All assays were performed in triplicate.

2.9. Mice

Female athymic BALB/c nude mice, 6–7 weeks old, were purchased from Charlsriver Co., Ltd. (Tokyo, Japan) and maintained in our animal facilities under specific pathogen-free conditions. All animal experiments were performed according to the Guidelines on Animal Experimentation as established by Juntendo University, School of Medicine.

2.10. In vivo tumorigenicity

SBC-3/OPN and SBC-3/NEO cells were harvested from the culture flask with 0.05% Trypsin-EDTA (Invitrogen), washed three times, resuspended in PBS. Cell viability was determined by trypan blue dye exclusion test and cells were inoculated subcutaneously (s.c.) into the left flank of nude mice (1×10^7 cells/mouse). To investigate whether tumor growth is mediated by the interaction between OPN and its receptor, the RMV-7 antibody was administered to SBC-3/OPN or SBC-3/NEO inoculated mice. Briefly, RMV-7 (200 μg/mouse) and control isotype-matched IgG (200 μg/mouse) were administered intraperitoneally from day 3 after inoculation three times a week for 3 weeks. TNP-470 (30 mg/kg) was also administered subcutaneously from day 7 twice a week for 3 weeks to reveal the involvement of angiogenesis in in vivo tumor growth. Tumor growth was measured with a digital caliper in two perpendicular diameters every week. Tumor volumes were calculated from the length (a) and width (b) by using the following formula:

volume (mm^3) = $ab^2/2$. Each group consisted of 10 mice. All experiments were performed twice.

2.11. Immunohistochemical staining

Histological sections were obtained from SBC-3/OPN and SBC-3/NEO tumor tissues resected from mice. After resection, tumor tissues were immediately embedded and frozen in Tissue-Tek OCD compound (Miles Laboratories, Elkhart, TN), and sections were cut at 4 μm thickness. Immunohistochemical staining for murine OPN and CD31 was performed as previously described [23]. To quantify apoptotic cell number in the tumor, we performed immunohistochemical staining for ssDNA. Briefly, the sections were fixed with 4% paraformaldehyde (PFA) and then incubated at 4°C overnight with rabbit anti-ssDNA antibody diluted to 1:400. Specific binding was detected through avidin-biotin peroxidase complex formation with biotin conjugated goat anti-rabbit IgG (Vectastain ABC kit, Vector, Burlingame, CA) and diaminobendizine (DAB) (Sigma, St. Louis, MI) as the substrate. Staining was absent when isotype-matched immunoglobulin was used as the control.

2.12. HUVEC proliferation assay

A 96-well flat bottom plastic assay plate (Corning, NY) was coated with recombinant mouse OPN (RD systems, Inc., CA; 10 μg/ml), polylysine (100 μg/ml) or BSA (10 mg/ml) in PBS and incubated overnight at 4°C. The plate was washed with PBS and non-specific adhesion sites were blocked with 1% BSA in PBS for 1 h at 37°C. After washing the wells with PBS, 5×10^3 cells in 100 μl of EGM-2 medium diluted with OPTI-MEM (Invitrogen) to 1/5 were seeded to each well. For some experiments, the HUVEC suspensions were pretreated with GRGDS peptide at the concentration of 100 μM or anti-human αvβ3 antibody at the concentration of 10 μg/ml for 1 h at 37°C. Then after 48 h incubation, 10 μl of 2-(2-methoxy-4-nitrophenyl)-3-(4-nitrophenyl)-5-(2,4-disulfophenyl)-2H-tetrazolium monosodium salt (WST-8, Dojindo, Kumamoto, Japan) was added to each well. The plate was further incubated at 37°C for 6 h for color development. Absorbance was measured at 450 nm on a microplate reader with microplate manager (Bio-Rad, Richmond, CA). All experiments were performed in triplicate.

2.13. Statistics

Statistical analysis was performed with analysis of variance (ANOVA). All data are presented as mean ± standard deviation. Differences between means were considered statistically significant at $P < 0.05$.

3. Results

3.1. Generation of stable transfectants that secretes murine OPN

BMGneo-mOPN or BMGneo were transfected into SBC-3 cells. Two OPN transfected SBC-3 clones (SBC-3/OPN#5 and SBC-3/OPN#6) and two control clones (SBC-3/NEO#1 and SBC-3/NEO#3) were constructed. To verify the expression of OPN and VEGF mRNA in transfectants, we conducted RT-PCR for OPN and VEGF, respectively. As shown in Fig. 1A, high levels of OPN mRNA expression were detected in the SBC-3/OPN cells, while there were no detectable expression levels observed in the SBC-3/NEO cells. For VEGF mRNA, there was no difference in the level of expression between SBC-3/OPN and SBC-3/NEO cells. Thus, transfection with OPN gene into SBC-3 cells does not affect the expression of other angiogenic inducers like VEGF mRNA. Secreted OPN protein from transfectants was confirmed with both western blot analysis and ELISA kit (Fig. 1B and C). OPN-transfected clones secreted significant amounts of OPN, while control clones did not. The clone SBC-3/OPN#5 secreted the high-

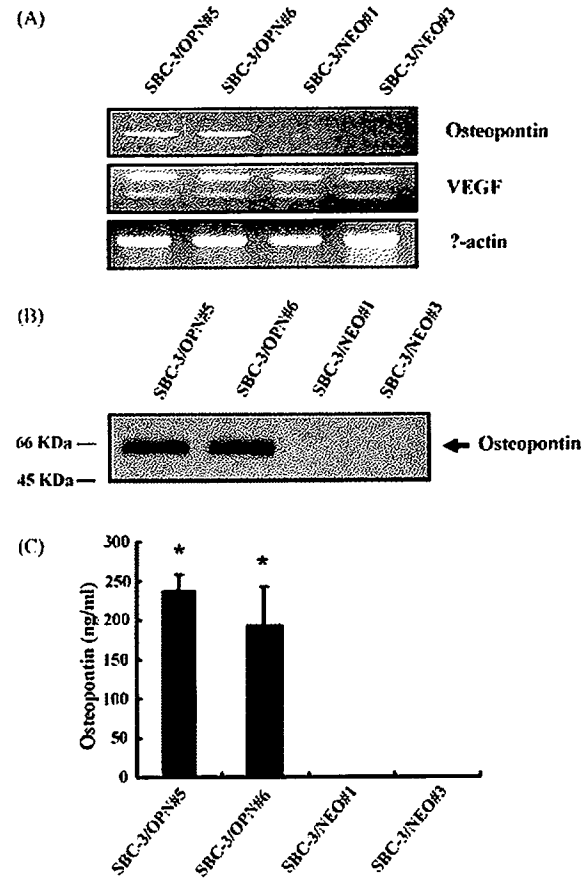

Fig. 1 (A) Expression of OPN and VEGF mRNA determined with RT-PCR analysis. Total RNAs were extracted from each clone and 1 μg of RNAs were subjected to RT-PCR analysis for OPN (top panel), VEGF (middle panel) and β-actin (bottom panel) expression. (B) Western blot analysis of secreted mouse OPN protein. Conditioned mediums from SBC-3/OPN and SBC-3/NEO clones were subjected to western blot analysis using polyclonal antibody against OPN. The arrow indicates the expression of OPN, and molecular standards are shown on the left in KD. (C) Secretion of OPN protein from SBC-3/OPN and SBC-3/NEO cells. Conditioned medium from each clones were collected and subjected to ELISA analysis. Note that the clone SBC-3/OPN#5 secreted the highest level of OPN protein into the culture medium. *$P < 0.05$ vs. SBC-3/NEO#1 and SBC-3/NEO#3.

est level of OPN protein into the culture medium. Therefore, we utilized this clone in the subsequential experiments.

3.2. In vitro cell growth rate of stable OPN-transfectant

Cells were seeded onto 96-well plates and the number of cells was quantified at specific time intervals with MTT assay. Cultured SBC-3/OPN and SBC-3/NEO cells displayed similar in vitro growth rates (data not shown).

3.3. Biological activity of OPN protein secreted from the transfectant

Since endothelial cell migration is essential for tumor angiogenesis, we conducted migration assay using HUVEC. Conditioned medium from SBC-3/OPN cells significantly stimulated HUVEC migration as compared with conditioned medium from SBC-3/NEO cells. Moreover, HUVEC migration toward the culture medium of SBC-3/OPN cells was almost completely suppressed with the addition of GRGDS peptide and anti-human αvβ3 antibody (Fig. 2). These results suggest that OPN secreted from SBC-3/OPN is actually biological active and stimulates HUVEC migration by interacting with αvβ3 integrin.

3.4. Effect of OPN transfection on colony formation

We evaluated whether transfection with OPN gene affects colony formation of SBC-3 cells in vitro with soft agar colony formation assay. As shown in Fig. 2B, there was no significant difference in the number of colonies between SBC-3/OPN and SBC-3/NEO cells. Thus, colony formation of SBC-3 cells in vitro was not affected by transfection with the OPN gene.

3.5. In vivo tumorigenecity of OPN transfectant

To investigate whether OPN has any role in tumor growth in vivo, SBC-3/OPN#5 clone and SBC-3/NEO#1 clone were injected subcutaneously into the left flank of the nude mice. As shown in Fig. 3 A and B, in contrast to the absence of any significant changes in in vitro cell growth, the in vivo growth rate of SBC-3/OPN#5 was significantly faster than that of the SBC-3/NEO#1 cells. We also tested in vivo tumor growth of the other SBC-3/OPN clone, SBC-3/OPN#6, to confirm its enhanced in vivo tumorigenecity. As expected, SBC-3/OPN#6 demonstrated enhanced in vivo tumor growth compared to SBC-3/NEO#1 (data not shown).

3.6. Expression of OPN protein in SBC-3/OPN and SBC-3/NEO tumors

To investigate whether enhanced tumor growth of SBC-3/OPN clones in vivo was mediated by secreted OPN, immunohistochemical staining for OPN was conducted. The OPN-positive cell number was significantly greater in the SBC-3/OPN induced tumor in comparison with that of the SBC-3/NEO tumor (Fig. 3C). These results suggest that

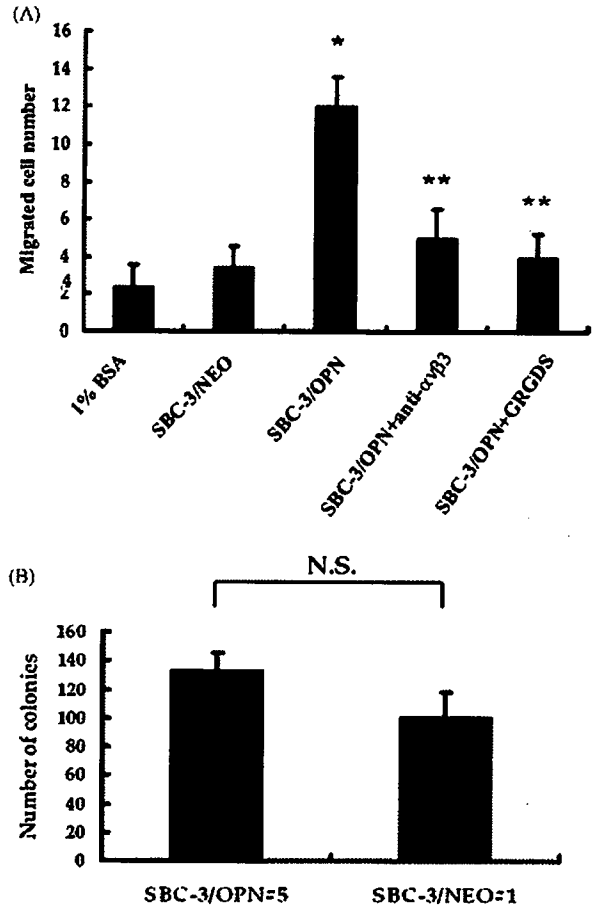

Fig. 2 (A) Migration of HUVEC toward conditioned medium from OPN-transfected cells. Cells were placed in the upper chamber and culture medium from SBC-3/NEO and SBC-3/OPN were added to the lower chamber. After 8 h incubation, cells that migrated through the porous filter were counted at ×200 magnification. Enhanced migration of HUVEC toward the culture medium from SBC-3/OPN was abrogated with the addition of either GRGDS peptide (100 μM) or anti-human αvβ3 antibody (10 μg/ml) to the upper chambers. Data are presented as mean ± S.D. $^{*}P < 0.0001$ vs. 1% BSA and SBC-3/NEO; $^{**}P < 0.001$ vs. SBC-3/OPN. (B) Soft-agar colony formation by SBC-3/OPN and SBC-3/NEO cells. Cells were seeded at an initial density of 5×10^3 cells into 6-well culture plates in triplicate in 0.3% agar. Colonies containing at least 50 cells were scored after 2 weeks of growth. Total colony per well were counted and presented as the mean ± S.D.

secreted OPN from SBC-3/OPN transfectants enhanced in vivo tumorigenesis.

3.7. Effect of OPN transfection on tumor angiogenesis

To investigate whether transfection with OPN gene results in increased tumor angiogenesis in vivo, we performed immunohistochemistry for CD31 and counted the microvessels in the SBC-3/OPN#5 and SBC-3/NEO#1 induced tumors of the nude mice. As shown in Fig. 4A, the number of CD31-

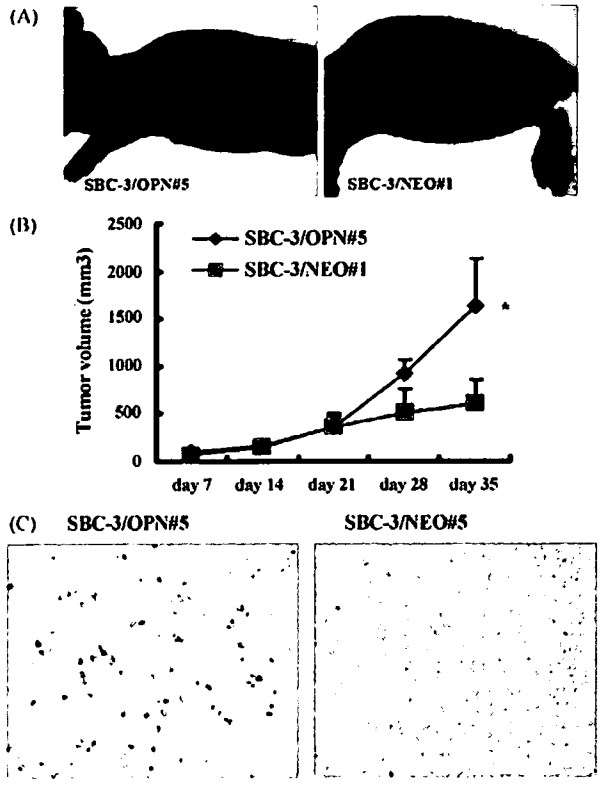

Fig. 3 Effect of OPN gene transfer into SBC-3 cells on tumor growth in mice. The SBC-3/OPN#5 and SBC-3/NEO#1 cells were inoculated s.c. into the left flanks of nude mice. (A) Representative photographs of the tumors at day 35 after inoculation with either the SBC-3/OPN#5 cells or the SBC-3/NEO#1 cells. (B) Tumors were measured with a digital caliper in two perpendicular diameters every week. The tumor volumes were calculated as described in Section 2. Each group consisted of 10 mice. $^{*}P<0.05$ vs. SBC-3/NEO#1. (C) Representative sections of OPN expression in tumors derived from SBC-3/OPN and SBC-3/NEO. Cryostat sections of tumors developing in nude mice were stained with anti-mouse OPN monoclonal antibody (original magnification ×400).

positive vascular endothelial cells was markedly increased in the SBC-3/OPN#5 induced tumor compared to that of the SBC-3/NEO#1 induced tumor. As shown in Fig. 4B, greater than tenfold the number of microvessels was identified in the SBC-3/OPN#5 induced tumor compared with the SBC-3/NEO#1 induced tumor. These results strongly imply that OPN upregulates tumor angiogenesis of SBC-3 cells in mice.

3.8. Effect of OPN transfection on tumor cell apoptosis

We evaluated whether transfection with OPN gene affects tumor cell apoptosis of SBC-3 cells in vivo with immunohistochemical staining for ssDNA. As shown in Fig. 4C, the number of apoptotic cells in the SBC-3/OPN induced tumor was not significantly different from that of the SBC-3/NEO induced tumor. These results suggest the apoptosis of SBC-3 cells in vivo was not affected by transfection with the OPN gene.

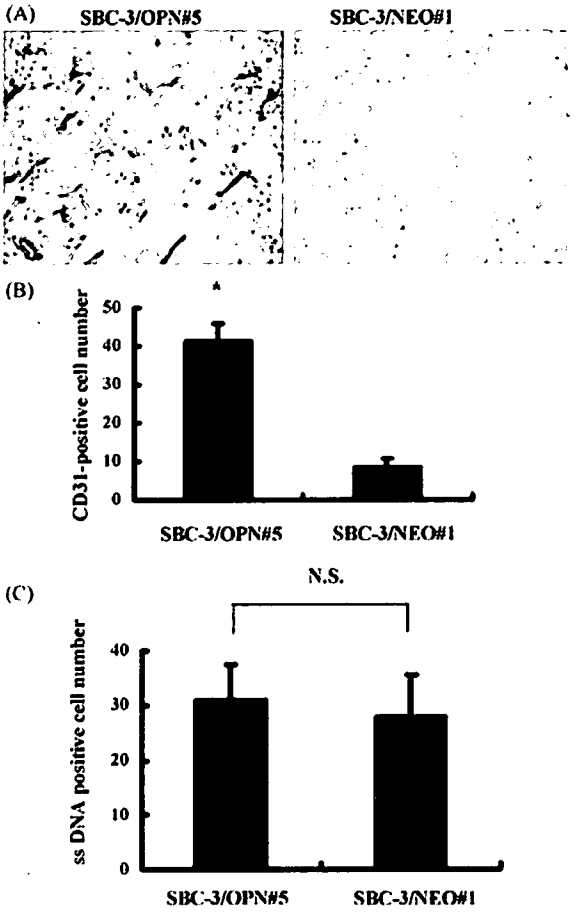

Fig. 4 (A and B) Vascularization of tumors derived from SBC-3/OPN#5 and SBC-3/NEO#1 cells. Cryostat sections of tumors developing in nude mice were stained with anti-CD31 monoclonal antibody. (A) Representative sections were depicted (×200). (B) Quantification of microvessel density in tumors. The number of CD31-positive microvessels in five fields of tumors that demonstrated the highest vascularity was counted at ×200 and presented as mean ± S.D. $^{*}P<0.001$ vs. SBC-3/NEO#1. (C) Quantification of ss DNA staining in SBC-3/OPN and SBC-3/NEO cells developed in nude mice. The number of ss DNA positive cells in SBC-3/OPN#5 tumor was not significantly different from that of SBC-3/NEO#1 tumor.

3.9. Effect of OPN on in vitro HUVEC proliferation

The endothelial cell proliferation is essential for tumor angiogenesis. Therefore, we performed HUVEC proliferation assay using recombinant mouse OPN protein. As shown in Fig. 5, immobilized OPN significantly stimulated HUVEC proliferation compared with immobilized polylysine and BSA. Interestingly, this enhanced HUVEC proliferation mediated by immobilized OPN was significantly inhibited with the addition of anti-human αvβ3 antibody or GRGDS peptide. These results are consistent with our finding that migration of HUVEC to OPN was mediated by αvβ3 integrin as shown in Fig. 2. Taken together, these findings imply the interaction between OPN and αvβ3 integrins on vascular endothelial cells may play an important role in tumor angiogenesis.

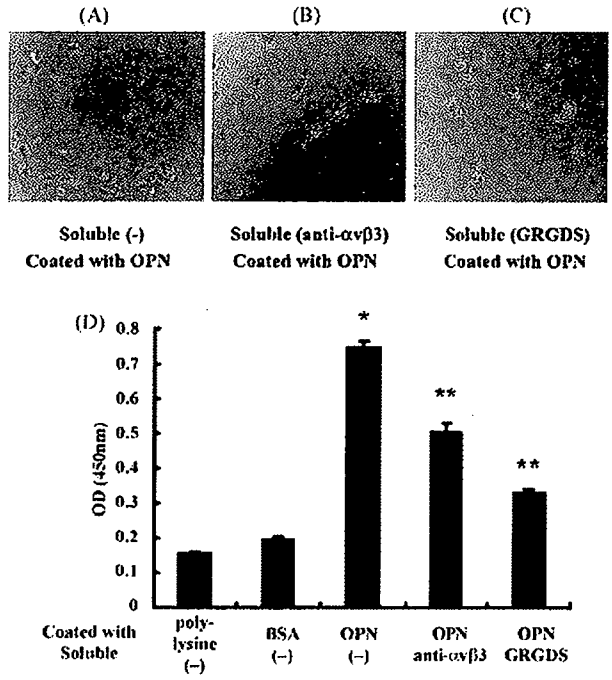

Fig. 5 Inhibitory effect of anti-αvβ3 antibody or RGD peptide on HUVEC proliferation mediated by OPN. (A–C) Representative microphotographs were depicted (×100). (D) Immobilized OPN significantly enhanced HUVEC proliferation and this enhancement was markedly suppressed by treatment with anti-αvβ3 antibody or RGD peptide. Data are presented as mean ± S.D. $^{*}P < 0.0001$ vs. coated with BSA, soluble (–); $^{**}P < 0.001$ vs. coated with OPN, soluble (–).

3.10. Effect of RMV-7 antibody or TNP-470 on growth of SBC-3/OPN tumor in vivo

Since the SBC-3/OPN#5 induced tumors revealed strong neovascularization and tumor growth, the SBC-3/OPN#5 induced tumors were treated with RMV-7 or anti-angiogenic agent, TNP-470, to investigate whether the accelerated SBC-3/OPN#5 tumor growth *in vivo* was directly associated with neovascularization mediated by the interaction between OPN and its receptor, αvβ3 integrin. As shown in Table 1, TNP-470 and RMV-7 administration significantly reduced *in vivo* tumor growth against SBC-3/OPN#5 cells with growth-inhibitory ratio (GIR) values (%) of 83.8% and 85.6%, respectively. In contrast to strong antitumor activity against SBC-3/OPN tumor, RMV-7 did not reveal any antitumor activity against the SBC-3/NEO tumor. These results suggest that the abrogation of the interaction between OPN and αvβ3 integrin could be an effective therapeutic modality in OPN-overexpressing lung cancer.

4. Discussion

OPN is a secreted multifunctional glycosylated phosphoprotein that is involved in tumor progression and metastasis through interaction with adhesion molecules such as integrins αvβ3, αvβ5, and αvβ1, and CD44 variants in a RGD sequence dependent or independent manner [24,25]. Angiogenesis plays a central role in the growth and metastasis of various cancers. The endothelial cell migration is dependent on their adhesive to extracellular matrix protein such as OPN through a variety of cell adhesion receptor including αvβ3 integrins [26]. It has been reported that overexpression of the αvβ3 integrin on tumor vasculature is associated with an aggressive phenotype of several solid tumor types [27,28]. Recent clinical studies also revealed that OPN, a ligand for αvβ3, overexpression is associated with tumor progression and poor survival of patients with lung cancer [17,18].

Table 1 Antitumor activity of RMV-7 or TNP-470 against SBC-3/OPN and SBC-3/NEO inoculated into nude mice

Cell line	Agent	Tumor volume (mm^3)	GIR (%)
SBC-3/OPN#5	TNP-470 (–)	506.9 ± 246.28	83.8
	TNP-470 (+)[b]	81.79 ± 34.4*	
	RMV-7 (–)	2272.45 ± 1126.73	85.6
	RMV-7 (+)[a]	326.35 ± 157.18**	
SBC-3/NEO#1	TNP-470 (–)	126.7 ± 27.98	27.1
	TNP-470 (+)[b]	92.36 ± 12.64	
	RMV-7 (–)	464.76 ± 167.49	3.6
	RMV-7 (+)[a]	448.17 ± 177.68	

Antitumor activity was evaluated in term of growth-inhibitory ratio (GIR, %), defined as [1 – (mean tumor volume of treated/mean tumor volume of control)] × 100 at day 32[a] after the first administration of RMV-7 or day 28[b] after the first administration of TNP-470. Data are presented as mean ± S.D.
* $P < 0.05$ vs. TNP-470 (–).
** $P < 0.05$ vs. RMV-7 (–).

In this study, we conducted *in vivo* tumorigenicity experiments using human lung cancer cell line, SBC-3 cells, to reveal whether interaction between OPN and its receptor αvβ3 plays a key role in tumor growth mediated by angiogenesis. The SBC-3 cell line was originally established from bone marrow aspirate of the 24-year-old male patient with small cell lung cancer [29]. Its subcutaneous implantability has been approved by Fukumoto et al. [30]. OPN-overexpressing SBC-3 cells significantly enhanced *in vivo* tumor growth compared to the control cells. Interestingly, *in vitro* cell growth rate and VEGF mRNA expression levels were similar among these cells. In contrast, transfection of SBC-3 cells with OPN gene significantly induced neovascularization *in vivo*. Apoptosis of SBC-3 cells *in vivo* and colony formation of SBC-3 cells *in vitro* were not affected by transfection with the OPN gene. These results imply that promotion of the tumor growth of SBC-3/OPN cells *in vivo* may be attributed to the hypervascularization induced by secreted OPN. In fact, recombinant human OPN protein enhanced HUVEC proliferation *in vitro*, and these effects of OPN were significantly suppressed with the addition of anti-αvβ3 integrin monoclonal antibody or RGD peptide. These results suggest that OPN is implicated in the process of angiogenesis by interacting with the αvβ3 integrin. In addition, we performed *in vivo* experiment to evaluate the metastatic effect of OPN. The cell suspensions of SBC-3/OPN or SBC-3/NEO cells were injected into a lateral tail vein of BALB/c nude mice. Unfortunately, we did not observe metastatic colonies in lungs. Although liver and kidney metastasis were observed, there

was no significant difference in the number of metastatic colonies in livers and kidneys between in SBC-3/OPN and SBC-3/NEO injected mice (data not shown).

The sustained growth of solid tumors is dependent on the vascular network, making tumor blood vessels a potential therapeutic target [3]. Since previous reports confirmed that OPN plays an important role in tumor progression and metastasis, various therapeutical trials targeting the interaction between OPN and its receptors have been proposed. Thalmann et al. reported that anti-OPN antibody inhibits the growth stimulatory effect of endogenous OPN for human prostate carcinoma cells [31]. In addition, a murine anti-human OPN antibody, which recognizes the RGD/thrombin cleavage region, inhibits the adhesion of MDA-MB-435 breast cancer cells to OPN [32]. Recent trials have used the siRNA technique to knock down OPN mRNA expression. Shevde et al. have demonstrated that suppression of OPN mRNA with siRNA reduced tumorigenecity of MDA-MB-435 breast cancer cells [33]. In addition, Wai et al. revealed that inhibition of OPN mRNA reduced metastatic potential in murine colon carcinoma cells [34]. Regarding anti-OPN receptor antibodies, Brooks et al. have reported that monoclonal antibody (LM609) against αvβ3 integrin induces apoptosis of the proliferative angiogenic blood vessel cells and leads to tumor regression in breast cancer [35]. However, there are no studies with regard to the therapeutic trials targeting OPN and its receptor in lung cancer animal models.

In the present study, we evaluated therapeutic efficacy of anti-αvβ3 integrin antibody (RMV-7) in OPN-overexpressing human lung cancer cells inoculated mice model. Treatment of mice with RMV-7 completely suppressed the *in vivo* tumor growth of SBC-3/OPN with GIR value of 85.6%, while growth rate of SBC-3/NEO *in vivo* was not attenuated by treatment with RMV-7. In the same way, anti-angiogenic agent, TNP-470, exhibited strong anti-tumor activity against SBC-3/OPN tumor with GIR value of 83.8%. These results suggest that interaction between OPN and αvβ3 integrin plays a crucial role for tumor growth induced by up-regulated angiogenesis of human lung cancer cells in mice and anti-αvβ3 antibody could be useful in anti-angiogenic treatment of human lung cancer.

Phase I study using vitaxin (humanized monoclonal anti-αvβ3 integrin antibody) has demonstrated its safety and potential activity in some human cancers. This study revealed that one patient demonstrated partial response and seven patients exhibited stable disease course among the 14 patients evaluated [36]. Recently, McNeel et al. reported phase I trial of a monoclonal antibody specific for αvβ3 integrin (MEDI-522) in patient with advanced multiple malignancies including lung cancer [37]. In their study, three patients with renal carcinoma demonstrated a prolonged and stable disease course among the 25 patients investigated. However, none of the patients with lung cancer revealed favorable therapeutic response. According to our previous report, OPN is predominantly expressed in NSCLC, but its expression level is variable [38]. In both phase I trials, they did not mention the issue of OPN expression in NSCLC. The reason why none of the patients with NSCLC revealed any response to treatment with anti-αvβ3 antibody might have been due to the low expression of OPN in NSCLC cells in these patients. In fact, administration of RMV-7 antibody did not reduce *in vivo* tumor growth in SBC-3/NEO cells inoculated mice in our study. These results suggest that intratumoral OPN expression could be a surrogate marker in the prediction of therapeutic response for treatment with anti-αvβ3 integrin antibody in lung cancer.

Conclusively, our study revealed that OPN is involved in tumor growth and angiogenesis of lung cancer by up-regulating vascular endothelial cell migration and proliferation via interacting with αvβ3 integrin. OPN and its receptor could be effective target molecules in the future for anti-angiogenic therapy of patients with lung cancer.

Conflict of interest

None.

References

[1] Bhattacharjee A, Richards WG, Staunton J, Li C, Monti S, Vasa P, et al. Classification of human lung carcinomas by mRNA expression profiling reveals distinct adenocarcinoma subclasses. Proc Natl Acad Sci USA 2001;98:13790–5.
[2] Chan DC, Earle KA, Zhao TL, Helfrich B, Zeng C, Baron A, et al. Exisulind in combination with docetaxel inhibits growth and metastasis of human lung cancer and prolongs survival in athymic nude rats with orthotopic lung tumors. Clin Cancer Res 2002;8:904–12.
[3] Folkman J. Angiogenesis in cancer, vascular, rheumatoid and other disease. Nat Med 1995;1:27–31.
[4] Folkman J, Shing Y. Angiogenesis. J Biol Chem 1992;267: 10931–4.
[5] Eliceiri BP, Cheresh DA. The role of alphav integrins during angiogenesis: insights into potential mechanisms of action and clinical development. J Clin Invest 1999;103:1227–30.
[6] Varner JA. The role of vascular cell integrins alpha v beta 3 and alpha v beta 5 in angiogenesis. Exs 1997;79:361–90.
[7] Patarca R, Saavedra RA, Cantor H. Molecular and cellular basis of genetic resistance to bacterial infection: the role of the early T-lymphocyte activation-1/osteopontin gene. Crit Rev Immunol 1993;13:225–46.
[8] Takahashi K, Takahashi F, Tanabe KK, Takahashi H, Fukuchi Y. The carboxyl-terminal fragment of osteopontin suppresses arginine-glycine-asparatic acid-dependent cell adhesion. Biochem Mol Biol Int 1998;46:1081–92.
[9] Agrawal D, Chen T, Irby R, Quackenbush J, Chambers AF, Szabo M, et al. Osteopontin identified as lead marker of colon cancer progression, using pooled sample expression profiling. J Natl Cancer Inst 2002;94:513–21.
[10] Chambers AF, Wilson SM, Kerkvliet N, O'Malley FP, Harris JF, Casson AG. Osteopontin expression in lung cancer. Lung Cancer 1996;15:311–23.
[11] Kim JH, Skates SJ, Uede T, Wong KK, Schorge JO, Feltmate CM, et al. Osteopontin as a potential diagnostic biomarker for ovarian cancer. JAMA 2002;287:1671–9.
[12] Tuck AB, Chambers AF. The role of osteopontin in breast cancer: clinical and experimental studies. J Mammary Gland Biol Neoplasia 2001;6:419–29.
[13] Tuck AB, O'Malley FP, Singhal H, Tonkin KS, Harris JF, Bautista D, et al. Osteopontin and p53 expression are associated with tumor progression in a case of synchronous, bilateral, invasive mammary carcinomas. Arch Pathol Lab Med 1997;121:578–84.
[14] Ue T, Yokozaki H, Kitadai Y, Yamamoto S, Yasui W, Ishikawa T, et al. Co-expression of osteopontin and CD44v9 in gastric cancer. Int J Cancer 1998;79:127–32.
[15] Senger DR, Ledbetter SR, Claffey KP, Papadopoulos-Sergiou A, Peruzzi CA, Detmar M. Stimulation of endothelial cell

migration by vascular permeability factor/vascular endothelial growth factor through cooperative mechanisms involving the alphavbeta3 integrin, osteopontin, and thrombin. Am J Pathol 1996;149:293–305.
[16] Shijubo N, Kojima H, Nagata M, Ohchi T, Suzuki A, Abe S, et al. Tumor angiogenesis of non-small cell lung cancer. Microsc Res Tech 2003;60:186–98.
[17] Donati V, Boldrini L, Dell'Omodarme M, Prati MC, Faviana P, Camacci T, et al. Osteopontin expression and prognostic significance in non-small cell lung cancer. Clin Cancer Res 2005;11:6459–65.
[18] Hu Z, Lin D, Yuan J, Xiao T, Zhang H, Sun W, et al. Overexpression of osteopontin is associated with more aggressive phenotypes in human non-small cell lung cancer. Clin Cancer Res 2005;11:4646–52.
[19] Takahashi F, Takahashi K, Okazaki T, Maeda K, Ienaga H, Maeda M, et al. Role of osteopontin in the pathogenesis of bleomycin-induced pulmonary fibrosis. Am J Respir Cell Mol Biol 2001;24:264–71.
[20] Takahashi K, Nakamura T, Koyanagi M, Kato K, Hashimoto Y, Yagita H, et al. A murine very late activation antigen-like extracellular matrix receptor involved in CD2- and lymphocyte function-associated antigen-1-independent killer-target cell interaction. J Immunol 1990;145:4371–9.
[21] Takahashi F, Akutagawa S, Fukumoto H, Tsukiyama S, Ohe Y, Takahashi K, et al. Osteopontin induces angiogenesis of murine neuroblastoma cells in mice. Int J Cancer 2002;98:707–12.
[22] Cui R, Takahashi K, Takahashi F, Tanabe KK, Fukuchi Y. Endostatin gene transfer in murine lung carcinoma cells induces vascular endothelial growth factor secretion resulting in up-regulation of in vivo tumorigenecity. Cancer Lett 2006;232:262–71.
[23] Hirama M, Takahashi F, Takahashi K, Akutagawa S, Shimizu K, Soma S, et al. Osteopontin overproduced by tumor cells acts as a potent angiogenic factor contributing to tumor growth. Cancer Lett 2003;198:107–17.
[24] Brown LF, Papadopoulos-Sergiou A, Berse B, Manseau EJ, Tognazzi K, Perruzzi CA, et al. Osteopontin expression and distribution in human carcinomas. Am J Pathol 1994;145:610–23.
[25] Weber GF, Ashkar S, Glimcher MJ, Cantor H. Receptor-ligand interaction between CD44 and osteopontin (Eta-1). Science 1996;271:509–12.
[26] Auerbach W, Auerbach R. Angiogenesis inhibition: a review. Pharmacol Ther 1994;63:265–311.
[27] Gasparini G, Brooks PC, Biganzoli E, Vermeulen PB, Bonoldi E, Dirix LY, et al. Vascular integrin alpha(v)beta3: a new prognostic indicator in breast cancer. Clin Cancer Res 1998;4:2625–34.
[28] Mitjans F, Sander D, Adan J, Sutter A, Martinez JM, Jaggle CS, et al. An anti-alpha v-integrin antibody that blocks integrin function inhibits the development of a human melanoma in nude mice. J Cell Sci 1995;108(Pt 8):2825–38.
[29] Miyamoto H. Establishment and characterization of an adriamycin-resistant subline of human small cell lung cancer cells. Acta Med Okayama 1986;40:65–73.
[30] Fukumoto H, Nishio K, Ohta S, Hanai N, Fukuoka K, Ohe Y, et al. Effect of a chimeric anti-ganglioside GM2 antibody on ganglioside GM2-expressing human solid tumors in vivo. Int J Cancer 1999;82:759–64.
[31] Thalmann GN, Sikes RA, Devoll RE, Kiefer JA, Markwalder R, Klima I, et al. Osteopontin: possible role in prostate cancer progression. Clin Cancer Res 1999;5:2271–7.
[32] Bautista DS, Xuan JW, Hota C, Chambers AF, Harris JF. Inhibition of Arg-Gly-Asp (RGD)-mediated cell adhesion to osteopontin by a monoclonal antibody against osteopontin. J Biol Chem 1994;269:23280–5.
[33] Shevde LA, Samant RS, Paik JC, Metge BJ, Chambers AF, Casey G, et al. Osteopontin Knockdown Suppresses Tumorigenicity of Human Metastatic Breast Carcinoma, MDA-MB-435. Clin Exp Metastasis 2006;23:123–33.
[34] Wai PY, Mi Z, Guo H, Sarraf-Yazdi S, Gao C, Wei J, et al. Osteopontin silencing by small interfering RNA suppresses in vitro and in vivo CT26 murine colon adenocarcinoma metastasis. Carcinogenesis 2005;26:741–51.
[35] Brooks PC, Stromblad S, Klemke R, Visscher D, Sarkar FH, Cheresh DA. Antiintegrin alpha v beta 3 blocks human breast cancer growth and angiogenesis in human skin. J Clin Invest 1995;96:1815–22.
[36] Gutheil JC, Campbell TN, Pierce PR, Watkins JD, Huse WD, Bodkin DJ, et al. Targeted antiangiogenic therapy for cancer using Vitaxin: a humanized monoclonal antibody to the integrin alphavbeta3. Clin Cancer Res 2000;6:3056–61.
[37] McNeel DG, Eickhoff J, Lee FT, King DM, Alberti D, Thomas JP, et al. Phase I trial of a monoclonal antibody specific for alphavbeta3 integrin (MEDI-522) in patients with advanced malignancies, including an assessment of effect on tumor perfusion. Clin Cancer Res 2005;11:7851–60.
[38] Zhang J, Takahashi K, Takahashi F, Shimizu K, Ohshita F, Kameda Y, et al. Differential osteopontin expression in lung cancer. Cancer Lett 2001;171:215–22.

Oncogene (2006), 1–11

www.nature.com/onc

ORIGINAL ARTICLE

Akt-dependent nuclear localization of Y-box-binding protein 1 in acquisition of malignant characteristics by human ovarian cancer cells

Y Basaki[1,2], F Hosoi[1,3,4], Y Oda[2], A Fotovati[4], Y Maruyama[4], S Oie[1,2], M Ono[1,3,4], H Izumi[5], K Kohno[5], K Sakai[6], T Shimoyama[6], K Nishio[6] and M Kuwano[1,4]

[1]Station-II for Collaborative Research, Kyushu University, Fukuoka, Japan; [2]Department of Anatomic Pathology, Graduate School of Medical Sciences, Kyushu University, Fukuoka, Japan; [3]Medical Biochemistry, Graduate School of Medical Sciences, Kyushu University, Fukuoka, Japan; [4]Research Center for Innovative Cancer Therapy, Kurume University, Kurume, Japan; [5]Department of Molecular Biology, University of Occupation and Environmental Health, Kitakyushu, Japan and [6]Pharmacology Division, National Cancer Center Research Institute, Tokyo, Japan

Y-box-binding protein 1 (YB-1), which is a member of the DNA-binding protein family containing a cold-shock domain, has pleiotropic functions in response to various environmental stimuli. As we previously showed that YB-1 is a global marker of multidrug resistance in ovarian cancer and other tumor types. To identify YB-1-regulated genes in ovarian cancers, we investigated the expression profile of YB-1 small-interfering RNA (siRNA)-transfected ovarian cancer cells using a high-density oligonucleotide array. YB-1 knockdown by siRNA upregulated 344 genes, including *MDR1*, *thymidylate synthetase*, *S100 calcium binding protein* and *cyclin B*, and downregulated 534 genes, including *CXCR4*, *N-myc downstream regulated gene 1*, *E-cadherin* and *phospholipase C*. Exogenous serum addition stimulated YB-1 translocation from the cytoplasm to the nucleus, and treatment with Akt inhibitors as well as Akt siRNA and integrin-linked kinase (ILK) siRNA specifically blocked YB-1 nuclear localization. Inhibition of Akt activation downregulated *CXCR4* and upregulated *MDR1* (*ABCB1*) gene expression. Administration of Akt inhibitor resulted in decrease in nuclear YB-1-positive cancer cells in a xenograft animal model. Akt activation thus regulates the nuclear translocation of YB-1, affecting the expression of drug-resistance genes and other genes associated with the malignant characteristics in ovarian cancer cells. Therefore, the Akt pathway could be a novel target of disrupting the nuclear translocation of YB-1 that has important implications for further development of therapeutic strategy against ovarian cancers.
Oncogene advance online publication, 30 October 2006; doi:10.1038/sj.onc.1210084

Keywords: Akt; microarray; ovarian carcinoma; Y-box-binding protein-1

Correspondence: Dr Y Basaki, Station-II for Collaborative Research, Kyushu University, 3-1-1 Maidashi, Higashi-ku, Fukuoka 812-8582, Japan.
E-mail: yubasaki@yahoo.co.jp
Received 28 February 2006; revised 25 August 2006; accepted 11 September 2006

Introduction

The Y-box-binding protein 1 (YB-1), which is a DNA/RNA-binding protein also known as dbpB, regulates transcription, translation, DNA damage repair and other biological processes in both the nucleus and cytoplasm (Matsumoto and Wolffe, 1998; Kohno *et al.*, 2003). In the cytoplasm, YB-1 regulates mRNA stability and translational regulation (Evdokimova *et al.*, 2001; Ashizuka *et al.*, 2002; Fukuda *et al.*, 2004), while in the nucleus, it plays a pivotal role in transcriptional regulation through specific recognition of the Y-box promoter element (Ladomery and Sommerville, 1995; Kohno *et al.*, 2003). Interaction of YB-1 with its cognate Y-box-binding site (inverted CCAAT box) is promoted by cytotoxic stimuli, including actinomycin D, cisplatin, etoposide, ultraviolet (UV) and heat shock, leading to the activation of a representative ABC transporter *MDR1/ABCB1* and DNA topoisomerase IIα genes (Asakuno *et al.*, 1994; Furukawa *et al.*, 1998; Ohga *et al.*, 1998). YB-1 also selectively interacts with damaged DNA or RNA, and protects from cytotoxic effects following cellular exposure to cisplatin, mitomycin C, UV and oxygen radicals (Ohga *et al.*, 1996; Ise *et al.*, 1999).

Royer and co-workers were the first to report that nuclear localization of YB-1 is associated with intrinsic *MDR1* expression in human primary breast cancer (Bargou *et al.*, 1997). Immunostaining analysis of various human cancers also supported this result, and showed that nuclear expression of activated YB-1 was closely associated with the acquisition of P-glycoprotein-mediated multidrug resistance (Kuwano *et al.*, 2004). YB-1 has also been shown to induce basal and 5-fluorouracil-induced expression of the major vault protein (*MVP/LRP*) gene, the promoter of which contains a Y-box (Stein *et al.*, 2005). In human malignancies, vault proteins are involved in acquiring drug resistance (Mossink *et al.*, 2003). Taken together, these findings suggest that nuclear localization of YB-1 might play a key role in the acquisition of global drug resistance through transcriptional activation of relevant genes and the repair of damaged DNA (Kuwano *et al.*, 2004).

The nuclear localization of YB-1 is required for transcription and DNA repair in response to various environmental stimuli, such as adenovirus infection (Holm *et al*., 2002), DNA-damaging agents, UV irradiation, hyperthermia (Stein *et al*., 2001) and serum stimulation (Lin-Nia *et al*., 2005). However, as a nucleocytoplasmic shuttling protein, it is important to understand which signalling molecules are involved in the translocation of YB-1 into the nucleus. Koike *et al*. (1997) first reported the possible role of protein kinase C in YB-1 nuclear translocation in cancer cells exposed to UV irradiation, and highlighted the importance of the YB-1 C-terminal region in cytoplasmic retention. Other studies have suggested the involvement of additional molecules: thrombin-mediated YB-1 nuclear translocation was shown to be inhibited by protein tyrosine phosphatase inhibitor in endothelial cells (Stenina *et al*., 2000), while Dooley *et al*. (2006) demonstrated the involvement of Jak1 in YB-1 nuclear translocation. Sutherland *et al*. (2005) recently reported that phosphorylation of YB-1 by Akt at serine 102 in the cold-shock domain is required for YB-1 nuclear translocation in cancer cells. Another mechanism for nuclear translocation of YB-1 was shown to be promoted by various cytotoxic anticancer agents, which trigger the proteolytic cleavage by the 20S proteasome of the YB-1 C-terminal fragment containing the cytoplasmic retention signal (Sorokin *et al*., 2005). In our present study, we have provided evidence that Akt activation is one of the mechanisms for nuclear translocalization of YB-1, and also that YB-1 regulates expression of various cell growth and malignant progression-related genes as well as global drug resistance-related genes including *MDR1*.

Results

Suppression of YB-1 leads to an enhancement of MDR-1 expression and decrease of CXCR-4 expression

We previously reported that YB-1 was expressed in the nucleus in almost 30% of serous ovarian cancers, and that YB-1 nuclear-positive patients had a poor prognosis (Kamura *et al*., 1999). As nuclear translocation of YB-1 is highly susceptible to environmental stimuli, we first examined whether the stress-inducing exogenous addition of serum could stimulate nuclear translocation of YB-1 in seven serum-deprived human ovarian cancer cell lines. Among the seven cell lines, nuclear YB-1 translocation was stimulated more than twofold in two: RMG-III and SKOV-3 (Figure 1a). In these two lines, serum incubation markedly enhanced Akt phosphorylation and increased translocation of YB-1 into the

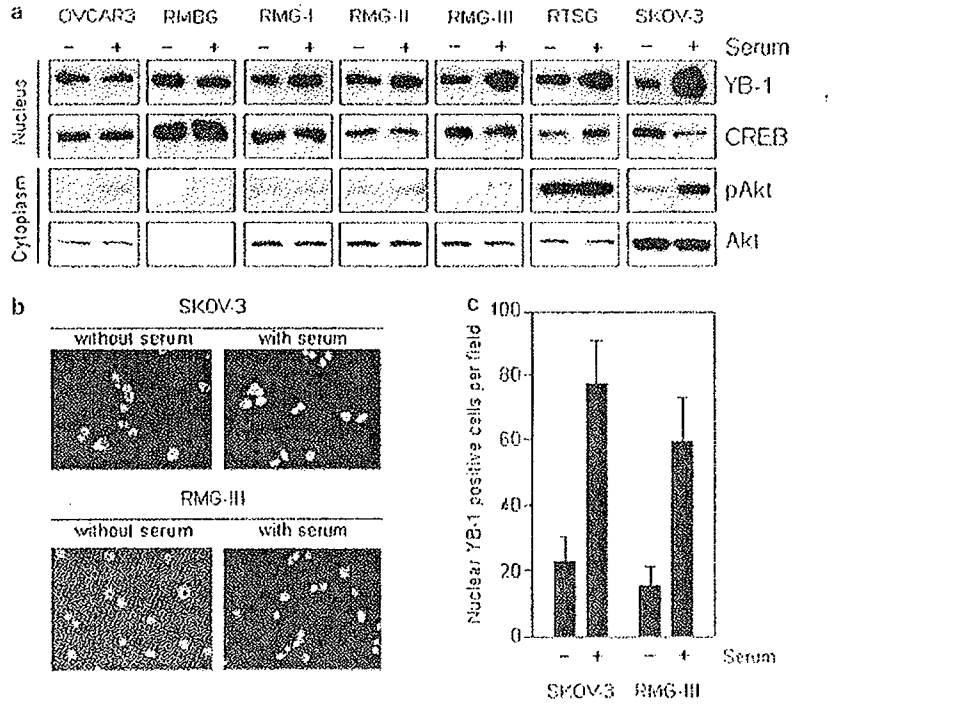

Figure 1 Levels of Akt phosphorylation and nuclear localization of YB-1 in ovarian cancer cell lines with or without serum stimulation. (a) Cytoplasmic and nuclear extracts were prepared 1 h after 10% serum stimulation. Anti-YB-1 and anti-CREB immunoblots were performed on nuclear extracts, and anti-pAkt and anti-Akt immunoblots were performed with cytoplasmic extracts. CREB and Akt are shown as a loading control. (b) Immunofluorescent staining of YB-1 in ovarian cancer cells. Cells stimulated with or without serum for 1 h were fixed and permeabilized, incubated at 4°C with the primary YB-1 antibody, then with the Alexa Fluor 546-labelled secondary antibody. (c) Quantitative analysis of YB-1 nuclear localization as shown in Figure 1b. Data are mean of three independent experiments; bars: ± s.d.

nucleus, as shown by immunofluorescense analysis (Figure 1b and c).

Although YB-1 is known to regulate the expression of several genes at the transcriptional level, the complete network of genes associated with YB-1 has not been elucidated. We therefore, explored the expression profile of YB-1 siRNA-treated SKOV-3 cells and mock-treated SKOV-3 cells using a high-density oligonucleotide microarray. We transfectd YB-1 siRNA into SKOV-3 cells at a concentration of 200 and 400 nM. Transfection of 200 nM YB-1 siRNA decreased expression of YB-1 mRNA by only 45%, whereas 400 nM YB-1 siRNA decreased by 70% (Figure 2). Of the 54 675 RNA transcripts and variants in the microarray, we identified 344 genes that were increased more than twofold and 534 genes that were decreased 0.5-fold or less in both 200 and 400 nM YB-1 siRNA-transfected cells (Supplementary Table S1). Upregulated genes were classified into 'cell cycle' ($P < 0.0001$), 'cytoskeleton organization and biogenesis' ($P = 0.0003$), 'cell growth and/or maintenance' ($P = 0.0005$), and GO SLIMS Biological Process' ($P = 0.0013$). Downregulated genes were classified into 'catalytic activity' ($P = 0.0007$) and 'transferase' ($P = 0.0010$). We selected 46 genes that we expected to be associated with drug resistance, cell growth, cancer malignant progression and cell signalling (Table 1), and chose three of these for further study: *MDR1*, *MVP/LRP* and chemokine (C-X-C motif) receptor 4 (*CXCR4*).

We used quantitative real-time PCR (QRT-PCR) to confirm whether expression of these three genes was modulated in YB-1 siRNA-transfected cells. Expression of *CXCR4* decreased by 67%, whereas expression of *MVP/LRP* was unaffected by the siRNA (Figure 2). *MDR1* expression was increased approximately 30-fold in 400 nM YB-1 siRNA-transfected cells compared with control siRNA-transfected cells. The results of QRT-PCR are broadly consistent with those of the microarray analysis.

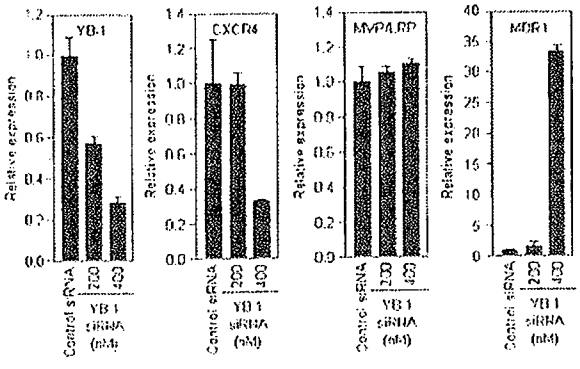

Figure 2 Effect of YB-1 knock down on expression of MDR1, MVP/LRP and CXCR4. SKOV-3 cells were treated with YB-1 siRNA for 48 h and then total RNA was prepared. QRT-PCR was performed for MDR1, MVP/LRP, CXCR4, YB-1 and housekeeping gene glyceraldehyde-3-phosphate dehydrogenase (GAPDH). The relative gene expression for each sample was determined using the formula $2^{-\Delta(\Delta C_T)} = 2^{-[(C_T(\text{gene}) - C_T(\text{GAPDH}))_{\text{Treated}} - (C_T(\text{gene}) - C_T(\text{GAPDH}))_{\text{Control}}]}$ which reflected target gene expression normalized to GAPDH levels. Data were mean of three independent experiments; bars ± s.d.

Pearson correlation and hierarchical cluster analysis of selected NCI-60 genes

We next examined a database containing the expression profile of the National Cancer Institute (NCI)-60 panel from the Developmental Therapeutics Program (http://www.dtp.nci.nih.gov/), shown as a log of mRNA expression level in the NCI screen. When the Pearson correlation coefficients were calculated, YB-1 was negatively correlated with *MDR1* expression, positively correlated with *CXCR4* expression and showed little correlation with *MVP/LRP* (Figure 3). Moreover, the hierarchical dendrogram of gene expression revealed that *YB-1* and *CXCR4* belong to the same cluster, whereas *MDR1* and *MVP/LRP* are clustered in a separate group (Figure 4). Together, these NCI-60 panels suggest that cellular levels of YB-1 negatively modulate expression of *MDR1* and positively regulate expression of *CXCR4*. In this cluster analysis, six ovarian cancer cell lines including SKOV-3 showed various correlation coefficiencies with YB-1 expression. Our oligonucleotide array analysis was performed only with SKOV-3, and correlation coefficiencies among ovarian cancer cell lines would depend upon which cell line was analysed.

Akt activity is prerequisite for nuclear translocation of YB-1and transcriptional regulation by YB-1

Phosphorylation of YB-1 by Akt is a necessary requirement for its translocation from the cytoplasm into the nucleus (Sutherland *et al*., 2005). We therefore investigated the effect of two inhibitors of Akt activation (LY294002 and 1L-6-hydroxymethyl-*chiro*-inositol 2(*R*)-2-*O*-methyl-3-*O*-octadecylcarbonate) on serum-stimulated SKOV-3 cells. Both Akt inhibitors markedly blocked the nuclear accumulation of YB-1, whereas treatment with inhibitors of MEK (U0126), p38MAPK (SB203580) and JNK (SP600125) had no effect on nuclear translocation (Figure 5a). In addition, phosphorylation of Akt was inhibited by LY294002 and octadecylcarbonate, but not by U0126, SB203580 and SP600125. Immunofluorescence analysis with a YB-1 antibody also demonstrated the predominant accumulation of YB-1 in the cytoplasm when treated with LY294002 and octadecylcarbonate (Figure 5b and c). As Akt inhibitors blocked the nuclear translocation of YB-1, we examined whether they could also affect expression of YB-1-regulated genes. *CXCR4* expression was found to be downregulated in a dose-dependent manner following treatment with the Akt inhibitors when determined by QRT-PCR analysis (Figure 5d). Treatment with Akt inhibitors upregulated the expression of *MDR1*, but not *MVP/LRP*.

SKOV-3 cells expressed high level of Akt1 protein, very low level of Akt2 protein, and no Akt3 protein when assayed by immunoblotting analysis (Figure 6a). We introduced siRNA targeting Akt or ILK into SKOV-3 cells at a concentration of 100 and 10 nM.

Table 1 List of genes differentially expressed in YB-1 siRNA-transfected SKOV-3 cells

Unigene	*Accession*	*Symbol*	*Description*	*Mean fold change*
Hs.489033	NM_000927	ABCB1	MDR1, ATP-binding cassette, sub-family B (MDR/TAP), member 1	2.46
Hs.369762	AB077208	TYMS	Thymidylate synthetase	1.71
Hs.198363	NM_018518	MCM10	MCM10 minichromosome maintenance deficient 10	1.70
Hs.405958	U77949	CDC6	CDC6 cell division cycle 6 homolog (*S. cerevisiae*)	1.66
Hs.442658	AB011446	AURKB	Aurora kinase B	1.65
Hs.516484	NM_005978	S100A2	S100 calcium-binding protein A2	1.48
Hs.23960	NM_031966	CCNB1	Cyclin B1	1.40
Hs.460184	AA604621	MCM4	MCM4 minichromosome maintenance deficient 4 (*S. cerevisiae*)	1.40
Hs.438720	AF279900	MCM7	MCM7 minichromosome maintenance deficient 7 (*S. cerevisiae*)	1.36
Hs.433168	NM_002960	S100A3	S100 calcium binding protein A3	1.33
Hs.115474	NM_002915	RFC3	Replication factor C (activator 1) 3, 38 kDa	1.28
Hs.122908	NM_030928	CDT1	DNA replication factor	1.28
Hs.329989	NM_005030	PLK1	Polo-like kinase 1 (*Drosophila*)	1.21
Hs.334562	NM_001786	CDC2	Cell division cycle 2, G1 to S and G2 to M	1.21
Hs.74034	NM_001753	CAV1	Caveolin 1, caveolae protein, 22 kDa	1.19
Hs.477481	NM_004526	MCM2	MCM2 minichromosome maintenance deficient 2, mitotin	1.16
Hs.284244	M27968	FGF2	Fibroblast growth factor 2 (basic)	1.10
Hs.179565	NM_002388	MCM3	MCM3 minichromosome maintenance deficient 3 (*S. cerevisiae*)	1.08
Hs.194698	NM_004701	CCNB2	Cyclin B2	1.01
Hs.506989	BC001866	RFC5	Replication factor C (activator 1) 5, 36.5 kDa	1.02
Hs.171596	NM_004431	EPHA2	EPH receptor A2	1.01
Hs.194143	NM_007294	BRCA1	Breast cancer 1, early onset	0.75
Hs.156346	NM_001067	TOP2A	Topoisomerase (DNA) II alpha 170 kDa	0.64
Hs.473163	NM_001719	BMP7	Bone morphogenetic protein 7 (osteogenic protein 1)	0.54
Hs.391464	NM_004996	ABCC1	MRP-1, ATP-binding cassette, sub-family C (CFTR/MRP), member 1	0.20
Hs.256301	NM_199249	MGC13170	Multidrug resistance-related protein	0.15
Hs.513488	NM_017458	MVP	Major vault protein	0.05
Hs.482526	NM_014886	TINP1	TGF beta-inducible nuclear protein 1	0.23
Hs.525557	NM_000295	SERPINA1	Serpin peptidase inhibitor, clade A (alpha-1 antiproteinase, antitrypsin), member	1.01
Hs.500466	BC003761	PTEN	Phosphatase and tensin homolog (mutated in multiple advanced cancers 1)	1.05
Hs.25292	NM_002229	JUNB	Jun B proto-oncogene	1.06
Hs.132225	AI934475	PIK3R1	Phosphoinositide-3-kinase, regulatory subunit, polypeptide 1 (p85 alpha)	−1.16
Hs.83169	NM_002421	MMP1	Matrix metalloproteinase 1 (interstitial collagenase)	−1.22
Hs.308999	NM_002742	PRKCM	Protein kinase C, mu	1.29
Hs.326035	NM_001964	EGR1	Early growth response 1	−1.29
Hs.2256	NM_002423	MMP7	Matrix metalloproteinase 7 (matrilysin, uterine)	1.32
Hs.197922	NM_018584	CaMKIINalpha	Calcium/calmodulin-dependent protein kinase II	1.36
Hs.132966	AA005141	MET	Met proto-oncogene (hepatocyte growth factor receptor)	1.39
Hs.208124	NM_000125	ESR1	Estrogen receptor 1	1.50
Hs.73793	M27281	VEGF	Vascular endothelial growth factor	1.53
Hs.381167	AW512196	SERPINB1	Serine (or cysteine) proteinase inhibitor, clade B (ovalbumin), member 1	1.70
Hs.413111	NM_002661	PLCG2	Phospholipase C, gamma 2 (phosphatidylinositol-specific)	−1.75
Hs.461086	NM_004360	CDH1	Cadherin 1, type 1, E-cadherin (epithelial)	−1.92
Hs.472793	AI631895	SGK2	Serum/glucocorticoid regulated kinase 2	−2.04
Hs.372914	NM_006096	NDRG1	*N-myc* downstream regulated gene 1	−2.34
Hs.421986	NM_001008540	CXCR4	Chemokine (C-X-C motif) receptor 4	−2.64

High-density oligonucleotide array was performed on 400 nM YB-1 siRNA-treated SKOV-3 cells and mock-treated cells. siRNA duplexes were transfected using LipofectAMINE2000 with Opti-MEM mediums. At 48 h after siRNA transfection, total RNA was prepared, and subjected to double-stranded cDNA synthesis and *in vitro* transcription. The labeled cRNA was applied to the oligonucleotide microarray.

respectively, and silencing effects of siRNA were analysed by immunoblotting (Figure 6a). In Akt siRNA almost completely silenced both Akt1 and Akt2, and siRNA for ILK, the upstream kinase for Akt, silenced ILK on protein level. Treatment with Akt siRNA and ILK siRNA resulted in a marked decrease in both pAkt expression and nuclear accumulation of YB-1 (Figure 6a). As both Akt and ILK siRNA blocked the nuclear translocation of YB-1, we examined their effects on expression of YB-1-regulated genes (Figure 6b). Treatment with Akt and ILK siRNA downregulated the expression of *CXCR4* gene, and upregulated the expression of *MDR1* gene. By contrast there appeared no marked effect on the expression of *MVP/LRP* and *YB-1* genes when treated with both siRNAs (Figure 6b).

Effect of LY294002 treatment on Akt phosphorylation and YB-1 nuclear localization in SKOV-3 xenograft

To further investigate the involvement of Akt in tumoural YB-1 nuclear localization, an *in vivo* xenograft